



**ON THE LMI OPTIMIZATION OF ACTIVE
AND SEMI ACTIVE VEHICLE
SUSPENSIONS**
Master of Science Thesis

Yousef HAJ HMIDI
Eskişehir, 2019

**ON THE LMI OPTIMIZATION OF ACTIVE AND SEMI ACTIVE
VEHICLE SUSPENSIONS**



Yousef HAJ HMIDI

MASTER OF SCIENCE THESIS

**Control and Command Systems Program
Supervisor: Asst. Prof. Dr. Semiha TÜRKAY**

**Eskişehir
Eskişehir Technical University
Institute of Graduate Programs
November 2019**

FINAL APPROVAL FOR THESIS

This thesis titled “ON THE LMI OPTIMIZATION OF ACTIVE AND SEMI ACTIVE VEHICLE SUSPENSIONS” has been prepared and submitted by Yousef HAJ HMIDI in partial fulfillment of the requirements in “Eskişehir Technical University Directive on Graduate Education and Examination” for the Degree of Master of Science in Electrical and Electronics Engineering Department has been examined and approved on 31/10/2019.

<u>Committee Members</u>	<u>Title, Name and Surname</u>	<u>Signature</u>
Member (Supervisor) :	Asst. Prof. Dr. Semiha TÜRKAY
Member :	Prof. Dr. Hüseyin AKÇAY
Member :	Assoc. Prof. Dr. Ahmet YAZICI

Prof. Dr. Murat TANIŞLI
Director of Institute of Graduate Programs

ABSTRACT

ON THE LMI OPTIMIZATION OF ACTIVE AND SEMI ACTIVE VEHICLE SUSPENSIONS

Yousef HAJ HMIDI

Department of Electrical and Electronics Engineering
Program in Control and Command Systems

Eskişehir Technical University, Institute of Graduate Programs, November 2019

Supervisor: Asst. Prof. Dr. Semiha TÜRKAY

In this study, a seven degrees of freedom full car model with linear parameters is derived, and three type of suspension systems, namely, passively, actively and semi actively suspended systems are reviewed to study car's vibration under random road excitation. The performance of suspension systems are determined by measuring the body accelerations, suspension travels and tire deflections to assess ride comfort and drive safety of the vehicle.

The active suspension system is controlled by single and multi objectives controllers and for each controller the vehicle behavior is observed. An LQG control is presented and a trade off in cost function between the output indices is made. A different scenarios for mixed H_2/H_∞ syntheses with regional pole placement constraints are generated and a dynamic output feedback solutions are solved using LMIs.

For the semi active suspension system, a classical approaches Skyhook, Groundhook and Hybrid are used to control the system since these approaches feature simplicity and lower cost compared to their active counterparts. A mixed H_2/H_∞ static output feedback controller realized by MR damper which utilizes the measurements of the velocity at each corner of sprung mass and the suspension travel speeds as feedback signals is designed for two types of Skyhook control law and solved via LMI to obtain the damping characteristics of MR dampers.

For the proposed controllers, the effectiveness is validated by simulation results and the achieved RMS responses are compared.

Keywords: Full car model, Active suspension, Semi active suspension, Road model, Multi-objective control, LMI optimization, H_∞ performance, H_2 performance, Static output feedback, Dynamic output feedback, State feedback, LQG control, Skyhook control, Groundhook control, Hybrid control.

ÖZET

AKTİF VE YARI-AKTİF ARAÇ SÜSPANSİYONLARI İÇİN LMI OPTİMİZASYONU

Yousef HAJ HMIDI

Elektrik-Elektronik Mühendisliği Anabilim Dalı
Kontrol ve Kumanda Sistemleri Bilim Dalı
Eskişehir Teknik Üniversitesi, Lisansüstü Eğitim Enstitüsü , Kasım 2019

Danışman: Dr. Öğr. Üyesi Semiha TÜRKAY

Bu çalışmada, doğrusal parametrelili, yedi serbestlik derecesine sahip tam-araç modeli türetilmiştir ve rassal yol girdileri ile uyarılmış bir aracın sırasıyla pasif, aktif ve yarı aktif süspansiyon tasarımı için yanıtı incelenmiştir. Süspansiyon sisteminin performansı, aracın yolcu konforu ve sürüş güvenliğini gösteren gövde ivmeleri, süspansiyon deformasyonları ve lastik yer değiştirmeleri ölçülerek gösterilmiştir.

Aktif süspansiyon sistemi tek veya çok amaçlı kontrolcüler ile kontrol edilmiştir ve her bir kontrolcü tasarımı için araç çıktı yanıtları incenmiştir. İlk olarak, maliyet fonksiyonunda yer alan çıktı endeksleri arasında uzlaşımı sağlayan Doğrusal Kare Gausyan (LQG) kontrolcüsü tasarlanmıştır. Daha sonra, bölgesel kutup yerleştirme kısıtlarını göz önüne alan karışık H_2/H_∞ kontrolcüsü farklı sürüş senaryoları için sentezlenmiştir ve dinamik geri besleme çıktı çözümleri doğrusal matris eşitsizlikleri (LMI) kullanılarak elde edilmiştir.

Son olarak, aktif sistemlere göre daha basit bir tasarıma sahip ve düşük maliyeti amaçlayan yarı-aktif süspansiyon sistemleri Skyhook, Groundhook and Hibrid klasik yaklaşımları kullanılarak tasarlanmıştır. Karışık H_2/H_∞ statik çıktı geri besleme kontrolcüsü, araç gövdesinin dört köşesinden elde edilen hız ve süspansiyon deformasyonu ölçümleri kullanılarak MR damper ile gerçekleştirilmiştir. Burada, Skyhook kontrol kuralı ve aktif LMI optimizasyonu MR damper'in karakteristik özelliklerini belirlemek için kullanılmıştır.

Sunulan aktif ve yarı aktif kontrolcüler için tasarım başarısı benzetim çalışmaları ve ölçeklendirilmiş RMS yanıtları ile gösterilmiştir.

Anahtar Sözcükler: Tam araç modeli, Aktif süspansiyon, Yarı-aktif süspansiyon, Yol modeli, Çok-amaçlı kontrol, LMI optimizasyonu, H_∞ performansı, H_2 performansı, Statik çıktı geri beslemesi, Dinamik çıktı geri beslemesi, Durum geri beslemesi, LQG kontrol, Skyhook kontrol, Groundhook kontrol, Hibrid kontrol.

ACKNOWLEDGMENTS

I would like to express my sincere gratitude to my supervisor, Asst. Prof. Dr. Semiha TÜRKAY, who has supported me throughout my research with her patience and supreme knowledge. I thank her for her guidance and encouragement, where good advice, support, and friendship has been invaluable on both academic and personal levels.

I gratefully acknowledge the scholarship financed by EU Scholarships Programme in coordination with YTB.



Yusef HAJ HMIDI

October, 2019

31/10/2019

**STATEMENT OF COMPLIANCE WITH ETHICAL PRINCIPLES
AND RULES**

I hereby truthfully declare that this thesis is an original work prepared by me; that I have behaved in accordance with the scientific ethical principles and rules throughout the stages of preparation, data collection, analysis and presentation of my work; that I have cited the sources of all the data and information that could be obtained within the scope of this study, and included these sources in the references section; and that this study has been scanned for plagiarism with “scientific plagiarism detection program” used by Eskişehir Technical University, and that “it does not have any plagiarism” whatsoever. I also declare that, if a case contrary to my declaration is detected in my work at any time, I hereby express my consent to all the ethical and legal consequences that are involved.

Yousef HAJ HMIDI

CONTENTS

	<u>Page</u>
TITLE PAGE	i
FINAL APPROVAL FOR THESIS	ii
ABSTRACT	iii
ÖZET	iv
ACKNOWLEDGMENTS	v
STATEMENT OF COMPLIANCE WITH ETHICAL PRINCIPLES AND RULES	vi
CONTENTS	vii
LIST OF TABLES	ix
LIST OF FIGURES	x
GLOSSARY OF SYMBOLS AND ABBREVIATIONS	xii
1. INTRODUCTION	1
1.1. Motivation	1
1.2. Background	2
1.3. Scope of The Study	5
2. REVIEW OF FULL CAR AND ROAD MODELING	6
2.1. Full Car Model	6
2.2. Road Model	10
3. ACTIVE SUSPENSION CONTROL DESIGN	12

3.1.	LQG Control	14
3.2.	Multi-Objective and Mixed Control	17
3.3.	Comparison of Active Suspension Results for Different Scenarios	21
4.	SEMI ACTIVE SUSPENSION CONTROL DESIGN	25
4.1.	Continuous Time System Discretization	25
4.2.	Skyhook Approach	26
4.3.	Groundhook Approach	31
4.4.	Hybrid Approach	33
5.	LMI OPTIMIZATION OF SKYHOOK CONTROL	39
5.1.	Conventional Skyhook Control Law	39
5.2.	Alternative Skyhook Control Law	44
5.3.	Frequency Domain Responses	47
6.	CONCLUSION AND FUTURE WORK	50
	REFERENCES	51

LIST OF TABLES

	<u>Page</u>
Table 2.1. The vehicle parameters for the full-car model (Türkay and Akçay, 2014)	7
Table 3.1. The stochastic responses of the passive and the LQG controlled suspensions.	17
Table 3.2. The stochastic responses of Problem 3.1 results for $\beta_1=30$, $\beta_2=0.01$, and $c=200$ (the rectangle length of LMI region)	22
Table 3.3. The stochastic responses of Problem 3.2 results for $\beta_1=1$, $\beta_2=1$, and $c=200$ (the rectangle length of LMI region).	23
Table 3.4. The stochastic responses of Problem 3.3 results for $c=200$ (the rectangle length of LMI region).	23
Table 3.5. The percentage changes of each active suspension design methodology over the passive one.	24
Table 5.1. The stochastic responses of the passive and Conventional skyhook suspensions.	43
Table 5.2. The stochastic responses of the passive and alternative skyhook suspension for $\alpha = 0.5$	48

LIST OF FIGURES

		<u>Page</u>
Figure 2.1.	Full car model.	6
Figure 3.1.	General control configuration.	14
Figure 4.1.	Ideal skyhook configuration of full car model.	27
Figure 4.2.	Heave suspension deflection frequency response for different values of $c_{sky_i}S$	28
Figure 4.3.	Ideal groundhook configuration of full car model.	31
Figure 4.4.	Heave tire deflection frequency response for different values of $c_{gro_i}S$	33
Figure 4.5.	Ideal hybrid configuration of full car model.	34
Figure 4.6.	Heave tire deflection frequency response for different values of $\alpha_i S$ for $c_{sky_i} = c_{gro_i} = 2c_i$	36
Figure 4.7.	Heave suspension deflection frequency response for different values of $\alpha_i S$ for $c_{sky_i} = c_{gro_i} = 2c_i$	36
Figure 4.8.	Roll tire deflection frequency response to roll input.	37
Figure 4.9.	Roll suspension travel frequency response to roll input.	37
Figure 4.10.	Roll acceleration frequency response to roll input.	37
Figure 5.1.	Relationship between RMS heave suspension travel and α	46
Figure 5.2.	Relationship between RMS heave tire deflection and α	46
Figure 5.3.	Relationship between RMS heave acceleration and α	47

Figure 5.4.	Relationship between RMS pitch acceleration and α	47
Figure 5.5.	Relationship between RMS roll acceleration and α	47
Figure 5.6.	Roll acceleration frequency response magnitudes of passive, Skyhook and active designed by solving Problem 3.1 suspension systems to the roll input: (solid) passive, (dashed) Skyhook and (dotted) active.	48
Figure 5.7.	Roll suspension travel frequency response magnitudes of passive, Skyhook and active designed by solving Problem 3.1 suspension systems to the roll input: (solid) passive, (dashed) Skyhook and (dotted) active.	48
Figure 5.8.	Roll tire deflection frequency response magnitudes of passive, Skyhook and active designed by solving Problem 3.1 suspension systems to the roll input: (solid) passive, (dashed) Skyhook and (dotted) active.	49

GLOSSARY OF SYMBOLS AND ABBREVIATIONS

I_n	Identity matrix
$0_{m \times n}$	m by n null matrix
A^T	Transpose of A
A^\perp	Orthogonal basis for the null space of A
$\bar{\sigma}$	Singular value
$diag(\cdot)$	Block diagonal matrix
$Trace(A)$	Trace of given square matrix A
$E(x)$	Expected value of random variable x
$\ T\ _2$	H_2 norm of T
$\ T\ _\infty$	H_∞ norm of T
PSD	Power Spectral Density
LQG	Linear Quadratic Gaussian
LQR	Linear Quadratic Regulator
LMI	Linear Matrix Inequalities
RMS	Root Mean Square
MR	Magneto Rheological
EH	Electro Hydraulic

1. INTRODUCTION

The aim of this chapter is to provide the reader with an introduction to the subjects conducted throughout the scope of this work. A general comparison of passive against active and semi active suspensions are presented in the motivation. A literature reviews are introduced in the background. The chapter ends with a contents of the thesis.

1.1. Motivation

A suspension system plays a central role in achieving ride comfort and drive safety for a vehicle. A good compromise between these objectives has been the driving force for advancements in automotive applications. Ride comfort associated to the amount of energy transmitted through the suspension into the vehicle body, where, lower the body acceleration, better is the ride comfort. Conversely, drive safety associated to the vertical motion of the tires and to the suspension travels, where, a firm and uninterrupted contact of wheels to road surface is desired for good road holding, and keeping the suspension travels below the maximum allowable stroke is required for preventing excessive suspension bottoming. Therefore, a lightly damped suspension provides good ride comfort but poor road holding, while a heavily damped suspension provides good road holding but poor ride comfort. So, the suspension system design requirements are:

- The ride comfort is related to accelerations of vehicle body which quantified by their RMS values that should be minimized especially in the frequency range (4-8)Hz where the human being is most sensitive for mechanical vibration (for Standardization, 1997).
- The road holding is related to dynamic tires loads which should be minimized and it happens by minimizing the RMS tire deflections to assure the vehicle safety.

- The suspension travels should not exceed the maximum allowable suspension which is constrained by the mechanical structure, usually the maximum suspension travel is $\pm 0.8m$.

The urgency to achieve a better compromise between the aforementioned conflicting requirements a several new advancements in automotive suspensions have been considered. A passive suspension is made up of a springs and a dampers, the energy is stored in the springs and dissipated through the dampers, where, these components have fixed characteristics. As a result, in this type of suspension the objectives can not be met simultaneously. However, this issue can be resolved by replacing the passive suspension with an active or a semi active suspension. An active suspension is composed of springs, dampers and force actuators, the energy can be dissipated or added to the suspension in controlled way. The force actuator is governed by controller, where several different controller design methods will be discussed later. The final type of suspension is a semi active suspension which consists of springs, ordinary dampers and semi active dampers. The semi active damper has the ability to change its damping characteristics by using a little amount of external power. Hence, it provides controlled real-time dissipation of energy. Semi active suspension is cheaper and less complex compered to the active one and more reliable when compared to the passive one. Thus, the semi active suspension is becoming more and more popular for commercial vehicles.

1.2. Background

Every so often in engineering a compromise involves the control deign process. The automotive suspensions design belongs to this category. Thus, for the sake of development of active and semi active suspensions to achieve a satisfied trade-off between ride comfort and drive safety, a number of analytical and experimental studies on vehicle suspensions have for many years been carried out and so are taking a considerable place in literature.

A number of different control techniques have been investigated for active suspension systems. In (Esmailzadeh and Fahimi, 1997) an optimal controller has been designed to minimize a quadratic cost function and then this optimal system has been controlled via Model Reference Adaptive Control. Due to practical limitation, all the states needed for the state feedback controller are not measurable, and thus an observer must be used in order to estimate the states. For this purpose, LQG control for half car model has been considered in (Taghirad and Esmailzadeh, 1998) and for full car model in (Chai and Sun, 2010). The robust control techniques such H_∞ has been studied to minimize the effect of road disturbances on vehicle and passengers, the tubulus linear electric motor as an actuator has been used and controlled by H_∞ control in (Kruczek and Stribrsky, 2004). To obtain a more appropriate model, the dynamics of driver's seat has been integrated to the car model and the resulted system has been synthesized by H_∞ state feedback control and H_∞ dynamic output feedback control in (Rizvi et al., 2018) . The suspension system includes an uncertain parameters, such as the sprung mass, whose value is dependent on the vehicle's load. In the presence of this problem, a load-dependent controller has been synthesized by using LMI techniques in (Gao et al., 2006). LMI based techniques handling multi-objective performances such as H_∞ performance with time domain constraints has been employed in (Chen and Guo, 2005). In (Türkay and Akçay, 2014) a mixed H_2/H_∞ synthesis problem considering a regional pole constraint has been formulated and reduced-order controller has been proposed which has achieved a better results compared to full-order one.

However, complexity and cost of active suspensions have restricted their uses (Esmailzadeh and Fahimi, 1997). Thus, the interest has been shifted toward semi active suspension designs. By virtue of industrial limitations on the semi active suspension's elements (dissipativity properties), the control design is harder compared to active counterpart. Many studies have been carried out on the classical comfort oriented control for semi active suspension, namely Skyhook control, in litterateurs.

A 2-states and continuous standard Skyhook control featuring MR damper has been presented in (Blanchard, 2003), (Liu et al., 2005), (Ihsan et al., 2008), (Abramov et al., 2009) and (Savaresi et al., 2010) since it represents a simple way to accomplish a good ride comfort. An improved version of Skyhook controls featuring MR damper has been used in (Sammier et al., 2003) for the quarter car Skyhook ideal configuration. For good performance and robustness properties the optimal techniques has been proposed. See, for example, (Poussot-Vassal et al., 2006). In (Du et al., 2005) an H_∞ static output feedback controller realized by MR damper has been adopted for quarter car model. A Model Predictive Control (MPC) has been exploited for semi active suspension in (Canale et al., 2006). The robust control design using Linear Parameter Varying (LPV) tool for semi active suspension has proposed and designed in (Poussot-Vassal et al., 2008) to minimize H_∞ performance while guaranteeing the semi active damper limitations (i.e. dissipative constraint and force limitations). Furthermore, the classical road holding oriented control for semi active suspension, namely Groundhook control, both cases 2-states and continuous strategies have been conducted in (Goncalves, 2001), (Ihsan et al., 2008) and (Savaresi et al., 2010) since they represent a simple way to reduce the road-tire forces. To take advantage of the benefits of both Skyhook and Groundhook an hybrid control has been proposed as an alternative policy for semi active suspension (Goncalves, 2001).

In most of the cited works above, the robust control law development for semi active suspensions have been carried out using a quarter-car model which in this model the roll and pitch motions of the vehicle can not be observed. Moreover, there have been no systematic methodology to obtain the damping characteristics for the semi active damper.

The main contribution of this study are then:

- Providing a benchmark to find these damping characteristics using static output feedback control solved via LMI optimization methods for full car model.

- Comparing behaviors of both LMI based multi-objective controlled active and semi active suspensions.

1.3. Scope of The Study

The contents of this thesis are as follows:

In Chapter 2, a comprehensive derivations of motion equations for the full car dynamics is obtained and re-represented as state space equations. Also, a road profile is produced and expressed as stationary Gaussian random processes to represent a typical road.

In Chapter 3, a different modern control techniques are introduced, employed and compared in term of RMS responses for the active suspension. A measurements needed for building an active controller are defined. An RMS performance indices are determined in order to evaluate the behavior of the road irregularities imposed vehicle under different control laws.

In Chapter 4, A classical semi active controls are conducted, and different measurements were defined to suit the proposed control methodologies. Since the actuating damping forces work in real time, a discretizing approach was introduced to convert a continuous time system into discrete time one.

The main contribution of this study is presented in Chapter 5 where a novel method based on LMI static output feedback control is proposed to optimally find the maximal damping coefficients of the semi active dampers. Both conventional and alternative Skyhook controls are studied.

The Chapter 6 concludes and sums up the results of the study and provides a recommendations for future work.

2. REVIEW OF FULL CAR AND ROAD MODELING

The contents of this chapter are as follows. In Section 2.1, a full car model is reviewed and a detailed derivation of motion equations are obtained to get a good approximation of real vehicle dynamics. In Section 2.2, the road model is estimated to provide a good analysis of the ride performance limitations of suspension systems (Türkyay and Akçay, 2005).

2.1. Full Car Model

The full car model with seven degrees of freedom intended for this study is shown in Fig.2.1. In the figure, the rear anti-roll bar is not shown. The vehicle body is

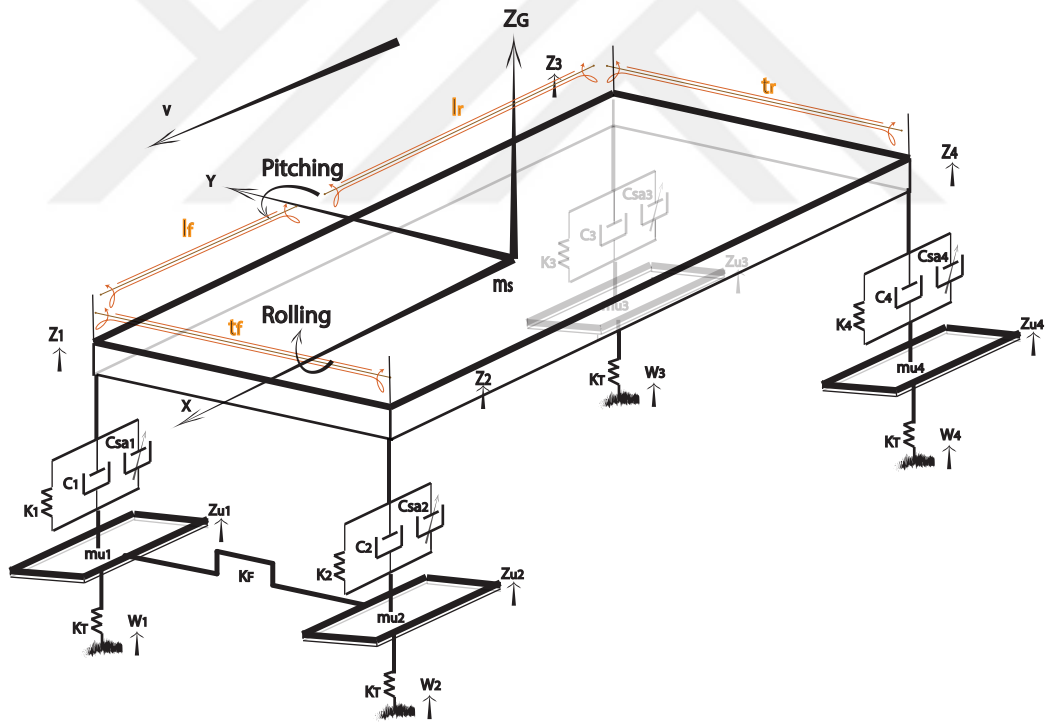


Figure 2.1. Full car model.

represented by the sprung mass m_s connected to the four unsprung masses m_{u_1} , m_{u_2} , m_{u_3} , and m_{u_4} , denoting the wheel masses at the front-left, the front-right, the rear-left, and the rear-right corners of the vehicle, respectively. The sprung mass is assumed to be rigid and has freedoms of motion in the heave, pitch, and roll direc-

tions, while the unsprung masses are free to bounce vertically with respect to the sprung mass. The suspension system between the sprung mass and the unsprung masses consists of linear passive suspension elements of springs and dampers in parallel with semi active dampers as shown in Fig.2.1 depicting semi active suspension system (or, force actuators in the active suspension system case). The tires are modeled as simple linear springs. Since the damping in the tires are typically very small, are neglected in this study. The pitch and the roll angles are assumed to be small. The vehicle parameter values are given in Table 2.1.

Table 2.1. *The vehicle parameters for the full-car model (Türkay and Akçay, 2014)*

Sprung mass	m_s	1460 kg
Roll moment of inertia	I_x	460 kgm ²
Pitch moment of inertia	I_y	2460 kgm ²
Left- and right-front unsprung masses	m_{u_1}, m_{u_2}	40 kg
Left- and right-rear unsprung masses	m_{u_3}, m_{u_4}	35.5 kg
Left- and right-front passive damping coefficients	c_1, c_2	1290 Ns/m
Left- and right-rear passive damping coefficients	c_3, c_4	1620 Ns/m
Left- and right-front suspension stiffnesses	k_1, k_2	19,960 N/m
Left- and right-rear suspension stiffnesses	k_3, k_4	17,500 N/m
Front auxiliary roll stiffness	K_F	19,200 Nrad/m
Rear auxiliary roll stiffness	K_R	0 Nrad/m
Tyre stiffnesses	k_T	17,500 N/m
Longitudinal distance from the front axle c.g. to the sprung mass c.g.	l_f	1.011 m
Longitudinal distance from the rear axle c.g. to the sprung mass c.g.	l_r	1.803 m
Front track width	t_f	1.522 m
Rear track width	t_r	1.510 m

Assuming the tires are in contact with road at all time that behave as point-contact followers, the equations of motion of this system are derived as follows:

Bouncing of the sprung mass:

$$\begin{aligned}
 m_s \ddot{z}_G = & -k_1(z_1 - z_{u_1}) - k_2(z_2 - z_{u_2}) - k_3(z_3 - z_{u_3}) - k_4(z_4 - z_{u_4}) \\
 & - c_1(\dot{z}_1 - \dot{z}_{u_1}) - c_2(\dot{z}_2 - \dot{z}_{u_2}) - c_3(\dot{z}_3 - \dot{z}_{u_3}) - c_4(\dot{z}_4 - \dot{z}_{u_4}) \\
 & - u_1 - u_2 - u_3 - u_4 \quad (2.1)
 \end{aligned}$$

Pitching of the sprung mass:

$$\begin{aligned}
I_y \ddot{\theta} = & k_1 l_f (z_1 - z_{u_1}) + k_2 l_f (z_2 - z_{u_2}) - k_3 l_r (z_3 - z_{u_3}) - k_4 l_r (z_4 - z_{u_4}) \\
& + c_1 l_f (\dot{z}_1 - \dot{z}_{u_1}) + c_2 l_f (\dot{z}_2 - \dot{z}_{u_2}) - c_3 l_r (\dot{z}_3 - \dot{z}_{u_3}) - c_4 l_r (\dot{z}_4 - \dot{z}_{u_4}) \\
& + l_f u_1 + l_f u_2 - l_r u_3 - l_r u_4 \quad (2.2)
\end{aligned}$$

Rolling of the sprung mass:

$$\begin{aligned}
I_x \ddot{\phi} = & k_1 \frac{t_f}{2} (z_1 - z_{u_1}) - k_2 \frac{t_f}{2} (z_2 - z_{u_2}) + k_3 \frac{t_r}{2} (z_3 - z_{u_3}) - k_4 \frac{t_r}{2} (z_4 - z_{u_4}) \\
& + c_1 \frac{t_f}{2} (\dot{z}_1 - \dot{z}_{u_1}) - c_2 \frac{t_f}{2} (\dot{z}_2 - \dot{z}_{u_2}) + c_3 \frac{t_r}{2} (\dot{z}_3 - \dot{z}_{u_3}) - c_4 \frac{t_r}{2} (\dot{z}_4 - \dot{z}_{u_4}) \\
& + \frac{t_f}{2} u_1 - \frac{t_f}{2} u_2 + \frac{t_r}{2} u_3 - \frac{t_r}{2} u_4 \quad (2.3)
\end{aligned}$$

Vertical direction for each wheel:

$$m_{u_i} \ddot{z}_{u_i} = k_1 (z_i - z_{u_i}) + c_i (\dot{z}_i - \dot{z}_{u_i}) - k_T (z_{u_i} - w_i) + u_i, \quad i=1, \dots, 4 \quad (2.4)$$

where:

- $z_1 = z_G - l_f \theta - \frac{t_f}{2} \phi$, $z_2 = z_G - l_f \theta + \frac{t_f}{2} \phi$, $z_3 = z_G + l_r \theta - \frac{t_r}{2} \phi$ and $z_4 = z_G + l_r \theta + \frac{t_r}{2} \phi$ are the vertical displacements at the corners of the car body,
- z_{u_i} , $i = 1, \dots, 4$ are the wheel displacements,
- w_i , $i = 1, \dots, 4$ are the road disturbances,
- z_G , θ and ϕ are the vertical displacement at the center of gravity, the pitch and the roll angles of the sprung mass, receptively, and
- u_i , $i = 1, \dots, 4$ are the forces applied by MR dampers (or by actuators in the actively suspended system) which will be determined later in this study.

For controller designing purpose the equation of motion should be expressed in state

space form as follow:

$$\dot{\hat{x}} = A_1 \hat{x} + B_1 w + B_2 u \quad (2.5)$$

where:

$\hat{x} = [\bar{x}^T \dot{\bar{x}}^T]^T$, $\bar{x} = [z_G \theta \phi z_{u_1} z_{u_2} z_{u_3} z_{u_4}]$ the state vector,

$$A_1 = \begin{pmatrix} 0_{7 \times 7} & I_7 \\ M^{-1}K & M^{-1}C \end{pmatrix}, B_1 = \begin{pmatrix} 0_{4 \times 7} & P^T M^{-T} \end{pmatrix}^T \text{ and } B_2 = \begin{pmatrix} 0_{4 \times 7} & W^T M^{-T} \end{pmatrix}^T$$

where:

$$C = \begin{pmatrix} -\Psi^T C_s \Psi & \Psi^T C_s \\ C_s \Psi & -C_s \end{pmatrix}, K = \begin{pmatrix} -\Psi^T K_s \Psi & \Psi^T K_s \\ K_s \Psi & -K_s - K_t \end{pmatrix}$$

$$M = \text{diag}(m_s, I_y, I_x, m_{u_1}, \dots, m_{u_4}), W = \begin{pmatrix} -\Psi & I_4 \end{pmatrix}^T \text{ and } P = \begin{pmatrix} 0_{4 \times 3} & K_t \end{pmatrix}^T$$

where:

$$\Psi = \begin{pmatrix} 1 & -l_f & -t_f/2 \\ 1 & -l_f & t_f/2 \\ 1 & l_r & -t_r/2 \\ 1 & l_r & t_r/2 \end{pmatrix}, C_s = \text{diag}(c_1, \dots, c_4), K_t = k_T I_4 \text{ and } K_s = \text{diag}(d_1, d_2)$$

where:

$$d_1 = \begin{pmatrix} k_1 + K_F/t_f^2 & -K_F/t_f^2 \\ -K_F/t_f^2 & k_2 + K_F/t_f^2 \end{pmatrix} \text{ and } d_2 = \begin{pmatrix} k_3 + K_R/t_r^2 & -K_R/t_r^2 \\ -K_R/t_r^2 & k_4 + K_R/t_r^2 \end{pmatrix}$$

Remark 2.1 For simplicity the front and rear auxiliary stiffness are excluded from the Eqs.2.1-2.4 while included in the state space Eq. 2.5.

2.2. Road Model

A four-wheeled vehicle traveling along a typical road vibrates due to imposed displacement excitation at each wheel, and thus induces dynamic forces on the road. The road displacements w_i , $i = 1, \dots, 4$ commonly are specified as a random process of a ground displacement power spectral density (Türkay and Akçay, 2010). The road random excitation processes may have time correlation between the front and the rear wheels and cross-correlation between the right and left wheels. However, in this study it will be assumed that the four road random excitation processes are independent of each other. This assumption guarantees the excitation of the three body motions. The ground displacement power spectral density is given by:

$$S_{w_i}(f) = |\tilde{G}(j2\pi f)|^2 \quad (2.6)$$

where f is the spatial frequency measured in *cycle/meter* and the transfer function \tilde{G} is minimum phase linear shape filter satisfies $w_i = \tilde{G}\eta_i$ where η_i are independent zero-mean spatial unit-intensity white noise processes. The filter \tilde{G} is translated to temporal domain as $\tilde{G}(s) = \tilde{G}(v^{-1}s)$. Hence, $S_{\eta_i}(2\pi f) = v^{-1}$ and $S_{w_i}(2\pi f) = |\tilde{G}_{w_i}(j2\pi f)|^2 S_{\eta_i}(2\pi f)$.

A first order shape filter $\tilde{G} = b_w(s + a_w)^{-1}$ is used to estimate the road PSD in Eq.2.6. By adjusting the filter parameter values as $a_w = 0.0572$ and $b_w = 0.0195$ a good estimation result has been obtained (Türkay and Akçay, 2010). In time domain the shape filter results in the road model as follow:

$$\dot{w}_i = -va_w w_i + \sqrt{vb_w} \zeta_i \quad (2.7)$$

and the state space representation of Eq.2.7 can be represented as:

$$\dot{x}_q = A_q x_q + B_q \zeta \quad (2.8)$$

$$w = C_q x_q + D_q \zeta \quad (2.9)$$

where: $A_q = -va_w I_4$, $B_q = I_4$, $C_q = \sqrt{vb_w} I_4$, $D_q = 0_{4 \times 4}$, ζ is a zero mean vector valued white noise process and v is a forward speed of the vehicle which is 20 *m/sec* in this study.

Now, by combining the Eq.s 2.5 and 2.8-2.9 the unified model of the vehicle model with the road model can be obtain, this model has the following augmented state space representation:

$$\dot{x} = Ax + B_\zeta \zeta + B_u u \quad (2.10)$$

where:

$$x = \begin{pmatrix} \hat{x} \\ x_q \end{pmatrix}, A = \begin{pmatrix} A_1 & B_1 C_q \\ 0_{4 \times 14} & A_q \end{pmatrix}, B_\zeta = \begin{pmatrix} B_1 D_q \\ B_q \end{pmatrix} \text{ and } B_u = \begin{pmatrix} B_2 \\ 0_{4 \times 4} \end{pmatrix}$$

and this augmented system will be considered in the controllers design procedure throughout this study.

3. ACTIVE SUSPENSION CONTROL DESIGN

This chapter is not about introducing a new suspension control methods. The sole purpose of this chapter is to provide a detailed study of synthesizing the suspension systems with modern control methods to build fully active suspension system.

Every control law designing technique requires regulated output. The variables of the regulated output vector r used for the suspension system are:

- The suspension travels ($z_i - z_{u_i}$, $i = 1, \dots, 4$) stacking in the vector r_1 .
- The tire deflections ($z_{u_i} - w_i$, $i = 1, \dots, 4$) stacking in the vector r_2 .
- The heave, the pitch, and the roll accelerations (\ddot{z}_d , $\ddot{\theta}$, and $\ddot{\phi}$, respectively) of driver located at longitudinal and lateral distances x_d and y_d , respectively, from center of gravity of the sprung mass stacking in the vector r_3 .

$$r = C_1 \hat{x} + D_{11} w + D_{12} u \quad (3.1)$$

where:

$$r = \begin{pmatrix} \underbrace{z_1 - z_{u_1} \dots z_4 - z_{u_4}}_{r_1} & \underbrace{z_{u_1} - w_1 \dots z_{u_4} - w_4}_{r_2} & \underbrace{\ddot{z}_d \ddot{\theta} \ddot{\phi}}_{r_3} \end{pmatrix}^T,$$

$$C_1 = \begin{pmatrix} \Psi & I_4 & 0_{4 \times 7} \\ 0_{4 \times 3} & I_4 & 0_{4 \times 7} \\ \Psi_d [0_{3 \times 7} & I_3 & 0_{3 \times 4}] A \end{pmatrix}, \quad D_{11} = \begin{pmatrix} 0_{4 \times 4} \\ -I_4 \\ \Psi_d [0_{3 \times 7} & I_3 & 0_{3 \times 4}] B_1 \end{pmatrix},$$

$$D_{12} = \begin{pmatrix} 0_{8 \times 4} \\ \Psi_d [0_{3 \times 7} & I_3 & 0_{3 \times 4}] B_2 \end{pmatrix} \text{ and } \Psi_d = \begin{pmatrix} 1 & -x_d & y_d \\ 0 & 1 & 0 \\ 0 & 0 & 1 \end{pmatrix}$$

After augmenting the road model states, the regulated output becomes:

$$r = C_r x + D_{r\zeta} \zeta + D_{ru} u \quad (3.2)$$

where:

$$C_r = \begin{pmatrix} C_1 & D_{11}C_q \end{pmatrix}, D_{r\zeta} = D_{11}D_q, D_{ru} = D_{12}$$

and the states are as defined in Chapter 2.

Minimizing \ddot{z}_d , $\ddot{\theta}$, and $\ddot{\phi}$ while keeping the suspension travels below the maximum allowable suspension stroke improves the ride comfort. Also, in order to guarantee a firm continual contact of the wheels to road, dynamic tire loads should not be greater than the static ones. Then, the design goal is to reduce the three sprung mass accelerations while keeping the constraints satisfied, such this problem is defined as multi objective control problem that can not be overcome using the passive suspension (Karnopp, 1986), but to some extent, it can be resolved by employing an active or semi active suspension.

With reference to the Fig. 3.1, for the design of a feedback law for the system $G(s)$, where $G(s)$ is the open-loop system (i.e. the passive suspension system), consider the measurements of the suspension travels and the vertical acceleration at each corner of the sprung mass, which can be written as:

$$y = C_y x + D_{y\zeta} \zeta + D_{yu} u \quad (3.3)$$

where:

$$y = \begin{pmatrix} z_1 - z_{u1} \dots z_4 - z_{u4} & \ddot{z}_1 \dots \ddot{z}_4 \end{pmatrix},$$

$$C_y = \begin{pmatrix} \Psi & -I_4 & 0_{4 \times 11} \\ [0_{4 \times 7} & \Psi & 0_{4 \times 8}]A \end{pmatrix}, D_{y\zeta} = \begin{pmatrix} 0_{4 \times 4} \\ [0_{4 \times 7} & \Psi & 0_{4 \times 8}]B_\zeta \end{pmatrix} \text{ and}$$

$$D_{yu} = \begin{pmatrix} 0_{4 \times 4} \\ [0_{4 \times 7} & \Psi & 0_{4 \times 8}]B_u \end{pmatrix}$$

The dynamic output feedback structure is:

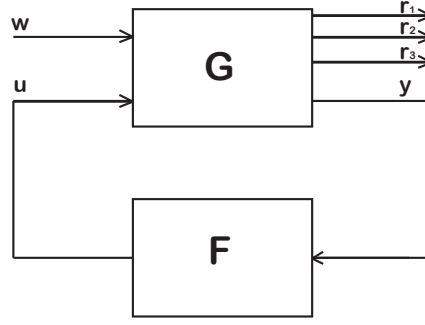


Figure 3.1. *General control configuration.*

$$\dot{x}_c = A_c x_c + B_c y \quad (3.4)$$

$$u = C_c x_c + D_c y \quad (3.5)$$

where the state space parameters A_c , B_c , C_c and D_c of the controller $F(s)$ are to be determined in this chapter to build the controlled system $T(s)$.

3.1. LQG Control

The Linear Quadratic Gaussian problem (LQG) is an optimal control problem where the objective is to design a controller that minimizes the quadratic cost function subject to linear system dynamics (Skogestad and Postlethwaite, 2007; Murray, 2009), provided that the system is stabilizable, detectable, and the process and measurement noises are zero-mean Gaussian processes. The solution for this problem known as Separation Principle, where, firstly finding the state feedback law gain that minimizes the cost function without taking into-account the noises (for the deterministic system), i.e. solving the LQR Problem and then, finding the Kalman filter gain that minimizes the estimation error and injecting the estimated states into the feedback law instead of the actual states, it is important to mention that the two solutions are independent of each other. The benefit of using Kalman filter is to estimate the states while are not available to measure in real world assuming process disturbance and measurement noise. The solution of the problem begins with finding the optimal control which minimizes the cost function (Esmailzadeh

and Fahimi, 1997):

$$J_{LQR} = \int_0^{\infty} (r(t)^T M_r r(t) + u(t)^T M_u u(t)) dt \quad (3.6)$$

where $M_r = M_r^T \geq 0$ and $M_u = M_u^T > 0$ are constant weighting matrices (design parameters) of the appropriate dimension, and choosing the matrices M_r and M_u plays a crucial role in system performances. Substituting Eq.3.2 into Eq.3.6 yields:

$$J_{LQR} = \int_0^{\infty} (x(t)^T Q x(t) + u(t)^T R u(t) + 2x(t)^T N u(t)) dt \quad (3.7)$$

with:

$$Q = C_r^T M_r C_r, R = D_{ru}^T M_r D_{ru} + M_u \text{ and } N = C_r^T M_r D_{ru}.$$

The weighting matrices are chosen as follows:

$$M_r = \text{diag}(\alpha_1, \dots, \alpha_{11}) * \text{diag}(\|G_{r(1)\zeta}\|_2^{-2}, \dots, \|G_{r(11)\zeta}\|_2^{-2})$$

$$M_u = \rho I_4$$

where $G_{r(i)\zeta}$ denotes the open loop transfer function from ζ to output $r(i)$ and added to normalize the outputs, while α_i are trade off parameters between the output indices, for $i = 1, \dots, 11$, and ρ is small constant allows to trade off the outputs versus the control forces, here $\rho = 10^{-8}$.

Then, the optimal solution is $u(t) = -K_r x(t)$, where:

$$K_r = R^{-1}(B_u^T X + N^T) \quad (3.8)$$

and $X = X^T \geq 0$ is the unique solution of the algebraic Riccati equation (Skogestad and Postlethwaite, 2007):

$$A^T X + X A - (X B_u + N) R^{-1} (X B_u + N)^T + Q = 0 \quad (3.9)$$

The next step now is to find Kalman filter gain that minimizes $E\{(x - \tilde{x})^T(x - \tilde{x})\}$, where the Kalman filter has dynamics as follows:

$$\dot{\tilde{x}} = A\tilde{x} + B_u u + K_f(y - \tilde{y}) \quad (3.10)$$

Then, the optimal choice of Kalman filter gain is:

$$K_f = Y C_y^T V^{-1} \quad (3.11)$$

where $Y = Y^T \geq 0$ is the unique solution of the algebraic Riccati equation (Skogestad and Postlethwaite, 2007):

$$Y A^T + A Y - Y C_y^T V^{-1} C_y Y + W = 0 \quad (3.12)$$

where $W = I_4$ and $V = 10^{-4} I_8$ are covariance matrices of process noise ζ and measurement noise n , respectively. By substituting the estimated states into control law the final control law can be obtained

$$u(t) = -K_r \tilde{x}(t) \quad (3.13)$$

where \tilde{x} is the optimal estimation of x . Finally, the closed loop dynamics are described by

$$\begin{pmatrix} \dot{x} \\ \dot{x} - \dot{\tilde{x}} \end{pmatrix} = \begin{pmatrix} A - B_u K_r & B_u K_r \\ 0 & A - K_f C_y \end{pmatrix} \begin{pmatrix} x \\ x - \tilde{x} \end{pmatrix} + \begin{pmatrix} B_\zeta & 0 \\ B_\zeta - K_f D_{y\zeta} & -K_f \end{pmatrix} \begin{pmatrix} \zeta \\ n \end{pmatrix}$$

$$r = \begin{pmatrix} C_r - D_{ru} K_r & D_{ru} K_r \end{pmatrix} \begin{pmatrix} x \\ x - \tilde{x} \end{pmatrix} + \begin{pmatrix} D_{r\zeta} & 0 \end{pmatrix} \begin{pmatrix} \zeta \\ n \end{pmatrix}$$

The stochastic responses of the passive and LQG controlled suspensions are displayed in Table 3.1.

Table 3.1. *The stochastic responses of the passive and the LQG controlled suspensions.*

RMS	$\ T_{r_1\zeta}\ _2$	$\ T_{r_2\zeta}\ _\infty$	$\ T_{r_3\zeta}\ _2$	$\ T_{\dot{z}_d\zeta}\ _2$	$\ T_{\ddot{\theta}\zeta}\ _2$	$\ T_{\ddot{\phi}\zeta}\ _2$
Passive	0.0752	0.009	4.7347	2.1738	1.3562	3.9816
LQG	0.0701	0.0089	3.1781	1.3656	0.8954	2.7265

Remark 3.1 *The RMS of a system output can be interpreted as H_∞ norm of the system, and as H_2 norm if the system is driven by zero-mean white noise processes.*

3.2. Multi-Objective and Mixed Control

The main drawbacks of LQG control are: the representing of process and measurement noises as Gaussian white noises which often they are not realistic, and the robustness is not being guaranteed (Zames, 1981), that has motivated researchers to shift towards H_∞ control. The main role of H_∞ control is to see whether the system performs according to desired criteria even in the worst case disturbances, such that H_∞ guarantees bounds on regulated outputs. Given a prescribed attenuation level γ_1 , a H_∞ suboptimal control problem is to design a controller $F(s)$ that internally stabilizes the closed-loop system and ensures:

$$\|T_{r\zeta}(s)\|_\infty = \max_{\zeta} \bar{\sigma}(T_{r\zeta}(j\omega)) \leq \gamma_1 \quad (3.14)$$

where $T_{r\zeta}(s) = C_{cl}(sI - A_{cl})^{-1}B_{cl} + D_{cl}$ is the closed-loop transfer matrix from ζ to r and $\bar{\sigma}(T_{r\zeta}(j\omega))$ is the maximal singular value of $T_{r\zeta}(j\omega)$.

In realistic control design problems one is not just confronted with a single-objective control problems but with multi-objectives ones should be satisfied simultaneously (Scherer and Weiland, 2000) such problems like the suspension system ones. Since the pure H_∞ synthesis can not capture all the design specifications, this leads to search for more powerful synthesis methods to render various objectives satisfied simultaneously. For instance, regulation against random disturbances or noise attenuation are more commonly expressed in H_2 synthesis terms (Gahinet et al., 1994). Moreover, standard H_∞ synthesis ensures only the closed-loop stabil-

ity without considering a direct placement of the closed-loop poles in more special regions of the left-half plane to perform a satisfactory time response. In addition, the avoidance of fast controller dynamics can be done by prohibiting large closed-loop poles (Chilali and Gahinet, 1996). One way of simultaneously tuning the H_∞ , H_2 performances, and transient behavior is therefore to combine H_∞ , H_2 , and pole placement objectives. Thus, multi-objectives synthesis is desirable to apply in practice and LMI theory provides a powerful tools to deal with such these problems. The LMI optimization problems have been modeled and solved using the MATLAB toolbox YALMIP (Löfberg, 2004).

These discussions lead to the definition of the mixed H_2/H_∞ control problem with regional pole placement which expressed in the following theorems.

Theorem 3.1 (H_∞ dynamic output feedback): (Caverly and Forbes, 2019)

There exists a controller in the form 3.4-3.5 such that the inequality $\|T_{r\zeta}(s)\|_\infty \leq \gamma_1$ holds if and only if the LMIs

$$\begin{pmatrix} N_{11} & A + A_n^T + B_u D_n C_y & B_w + B_u D_n D_{y\zeta} & (C_r Y_1 + D_{ru} C_n)^T \\ * & A^T X_1 + X_1 A + B_n C_y + (B_n C_y)^T & X_1 B_\zeta + B_n D_{y\zeta} & (C_r + D_{ru} D_n C_y)^T \\ * & * & -\gamma_1 I & (D_{r\zeta} + D_{ru} D_n D_{y\zeta})^T \\ * & * & * & -\gamma_1 I \end{pmatrix} < 0,$$

$$\begin{pmatrix} Y_1 & I \\ * & X_1 \end{pmatrix} > 0$$

hold, where $N_{11} = AY_1 + Y_1 A^T + B_u C_n + (B_u C_n)^T$ and the matrices A_n , B_n , C_n , D_n and the symmetric matrices X_1 , Y_1 are the variables of appropriate dimensions.

Theorem 3.2 (H_2 dynamic output feedback): (Scherer and Weiland, 2000)

There exists a controller in the form 3.4-3.5 such that the inequality $\|T_{r\zeta}(s)\|_2 \leq \gamma_2$

holds if and only if the LMIs

$$\begin{pmatrix} N_{11} & A + A_n^T + B_u D_n C_y & B_w + B_u D_n D_{y\zeta} \\ * & A^T X_1 + X_1 A + B_n C_y + (B_n C_y)^T & X_1 B_\zeta + B_n D_{y\zeta} \\ * & * & -\gamma_2 I \end{pmatrix} < 0,$$

$$\begin{pmatrix} Y_1 & I & (C_r Y_1 + D_{ru} C_n)^T \\ * & X_1 & (C_r + D_{ru} D_n C_y)^T \\ * & * & Z \end{pmatrix} > 0$$

and

$$D_{r\zeta} + D_{ru} D_n D_{y\zeta} = 0,$$

$$\text{Trace}(Z) < \gamma_2^2$$

hold, where $N_{11} = AY_1 + Y_1 A^T + B_u C_n + (B_u C_n)^T$ and the matrices A_n , B_n , C_n , D_n and the symmetric matrices X_1 , Y_1 , Z are the variables of appropriate dimensions.

By defining LMI constraints on the Lyapunov matrix a pole assignment in convex regions of the left-half plane can be determined (Scherer et al., 1997). In this study the open rectangle convex region is selected and it has been taken from (Türkay and Akçay, 2014) work.

Theorem 3.3 (Regional pole constraints): *The closed loop system has poles in the LMI region $\{z = a + jb, -c < a < 0, |b| < c\}$ if and only if the LMIs*

$$\begin{pmatrix} M_{11} + M_{11}^T & 0 \\ * & -2cX_v - M_{11} - M_{11}^T \end{pmatrix} < 0,$$

$$\begin{pmatrix} -2cX_v & M_{11}^T - M_{11} \\ * & -2cX_v \end{pmatrix} < 0$$

hold, where

$$M_{11} = \begin{pmatrix} AY_1 + B_u C_n & A + B_u D_n C_y \\ A_n & X_1 A + B_n C_y \end{pmatrix},$$

$$X_v = \begin{pmatrix} Y_1 & I \\ * & X_1 \end{pmatrix}$$

where the matrices A_n , B_n , C_n , D_n and the symmetric matrices X_1 , Y_1 are the variables of appropriate dimensions.

Remark 3.2 The symbol $*$ generically denotes the transposition of symmetric block of partitioned symmetric matrix.

Then, the state space parameters of the controller $F(s)$ in the form 3.4-3.5 are recovered by:

$$\begin{aligned} A_c &= A_k - B_c(I - D_{yu}D_c)^{-1}D_{yu}C_c & B_c &= B_k(I - D_{yu}D_c) \\ C_c &= (I - D_cD_{yu})C_k & D_c &= (I + D_kD_{yu})^{-1}D_k \end{aligned}$$

where:

$$\begin{aligned} A_k &= X_2^{-1}(A_n - B_n C_y Y_1 - X_1 B_u C_n - X_1(A - B_u D_n C_y)Y_1)Y_2^{-T} \\ B_k &= X_2^{-1}(B_n - X_1 B_u D_n) \\ C_k &= (C_n - D_n C_y Y_1)Y_2^{-T} \\ D_k &= D_n \end{aligned}$$

and the matrices X_2 and Y_2 satisfy $X_2 Y_2 = I - X_1 Y_1$.

The state space realization of the closed loop transfer matrix $T_{r\zeta}(s)$ is:

$$\begin{aligned}
A_{cl} &= \begin{pmatrix} A + B_u D_c (I - D_{yu} D_c)^{-1} C_y & B_u (I + D_c (I - D_{yu} D_c)^{-1} D_{yu}) C_c \\ B_c (I - D_{yu} D_c)^{-1} C_y & A_c + B_c (I - D_{yu} D_c)^{-1} D_{yu} C_c \end{pmatrix} \\
B_{cl} &= \begin{pmatrix} B_\zeta + B_u D_c (I - D_{yu} D_c)^{-1} D_{y\zeta} \\ B_c (I - D_{yu} D_c)^{-1} D_{yw} \end{pmatrix} \\
C_{cl} &= \begin{pmatrix} C_r + D_{ru} D_c (I - D_{yu} D_c)^{-1} C_y & D_{ru} (I + D_c (I - D_{yu} D_c)^{-1} D_{yu}) C_c \end{pmatrix} \\
D_{cl} &= D_{r\zeta} + D_{ru} D_c (I - D_{yu} D_c)^{-1} D_{y\zeta}
\end{aligned}$$

When the aforementioned theorems solved in one synthesizing problem, the Lyapunov matrix and the LMI variables should be the same, such that various design objectives meet simultaneously. For example, minimizing the H_2 norm of the transfer matrix from the exogenous input to one group of the partitioned performance output (applying the Theorem 3.2) while ensuring the H_∞ norm of the transfer matrix from the exogenous input to another group of the partitioned performance output does not exceed a prescribed value (applying the Theorem 3.1), and forcing the closed loop poles into specified LMI region such as the one defined in Theorem 3.3. A different scenarios of multi-objective synthesis will be discussed in the next section to get a satisfactory performance of the suspension system.

3.3. Comparison of Active Suspension Results for Different Scenarios

For the suspension system 2.10 with performance output 3.2 and measurements 3.3 a different multi-objective control design scenarios were presented to analyze the potentiality of the trade-offs among the ride comfort, suspension rattle-space compactness, and road holding characteristics. These scenarios summarized in the next problems.

Let us consider the problem of minimizing the heave, pitch and roll accelera-

tions of the driver and suspension travels, and constraining the dynamic tire loads such that does not exceed the static tire loads, and adding pole placement constraint to prevent high gained controller.

Problem 3.1 *Given H_∞ norm bound γ_1 and a subset of the open left-half plane D , design a controller $F(s)$ that minimizes*

$$\beta_1 \|T_{r_1\zeta}(s)\|_2 + \beta_2 \|T_{r_3\zeta}(s)\|_2$$

subject to $\|T_{r_2\zeta}(s)\|_\infty \leq \gamma_1$ and assigns the closed-loop poles in D .

The LMIs based solution found using Theorem 3.2 to optimally minimize the weighted sum $\beta_1 \|T_{r_1\zeta}(s)\|_2 + \beta_2 \|T_{r_3\zeta}(s)\|_2$ where, β_1 and β_2 are fixed real weights and the larger β_i , the more weight is put on penalizing the corresponding norm. Moreover, the solution is constrained by: H_∞ norm bound γ_1 on $\|T_{r_2\zeta}(s)\|_\infty$ which γ_1 is usually H_∞ norm of the corresponding passive (open-loop) system and this done by solving Theorem 3.1, and closed-loop poles assignment in the LMI region which defined in Theorem 3.3. The results shown in Table 3.2.

Table 3.2. *The stochastic responses of Problem 3.1 results for $\beta_1=30$, $\beta_2=0.01$, and $c=200$ (the rectangle length of LMI region)*

RMS	$\ T_{r_1\zeta}\ _2$	$\ T_{r_2\zeta}\ _\infty$	$\ T_{r_3\zeta}\ _2$	$\ T_{z_d\zeta}\ _2$	$\ T_{\ddot{\theta}\zeta}\ _2$	$\ T_{\ddot{\phi}\zeta}\ _2$
Passive	0.0752	0.009	4.7347	2.1738	1.3562	3.9816
Problem 3.1	0.0725	0.0074	2.4697	1.3161	1.0928	1.7813

Let us consider the problem of minimizing the suspension travels and the dynamic tire loads, and constraining the heave, pitch, and roll accelerations of the driver with satisfied bound, and adding pole placement constraint to prevent high gained controller.

Problem 3.2 *Given H_2 norm bound γ_2 and a subset of the open left-half plane D ,*

design a controller $F(s)$ that minimizes

$$\beta_1 \|T_{r_1\zeta}(s)\|_2 + \beta_2 \|T_{r_2\zeta}(s)\|_\infty$$

subject to $\|T_{r_3\zeta}(s)\|_2 \leq \gamma_2$ and assigns the closed-loop poles in D .

Employing the Theorems 3.1, 3.2, and 3.3 the solution found and shown in Table 3.3.

Table 3.3. The stochastic responses of Problem 3.2 results for $\beta_1=1$, $\beta_2=1$, and $c=200$ (the rectangle length of LMI region).

RMS	$\ T_{r_1\zeta}\ _2$	$\ T_{r_2\zeta}\ _\infty$	$\ T_{r_3\zeta}\ _2$	$\ T_{\dot{z}_d\zeta}\ _2$	$\ T_{\ddot{\theta}\zeta}\ _2$	$\ T_{\ddot{\phi}\zeta}\ _2$
Passive	0.0752	0.009	4.7347	2.1738	1.3562	3.9816
Problem 3.2	0.0684	0.0708	1.2017	0.7322	0.6847	0.6626

Let us consider the problem of minimizing the heave, pitch, and roll accelerations of the driver, while constraining the suspension travels and the dynamic tire loads with satisfied bounds, and adding pole placement constraint to prevent high gained controller.

Problem 3.3 Given H_∞ and H_2 norm bounds γ_1 and γ_2 , respectively, and a subset of the open left-half plane D , design a controller $F(s)$ that minimizes $\|T_{r_3\zeta}(s)\|_2$ subject to $\|T_{r_1\zeta}(s)\|_\infty \leq \gamma_1$ and $\|T_{r_2\zeta}(s)\|_2 \leq \gamma_2$ and assigns the closed-loop poles in D .

Employing the Theorems 3.1, 3.2, and 3.3 the solution found and displayed in Table 3.4.

Table 3.4. The stochastic responses of Problem 3.3 results for $c=200$ (the rectangle length of LMI region).

RMS	$\ T_{r_1\zeta}\ _2$	$\ T_{r_2\zeta}\ _\infty$	$\ T_{r_3\zeta}\ _2$	$\ T_{\dot{z}_d\zeta}\ _2$	$\ T_{\ddot{\theta}\zeta}\ _2$	$\ T_{\ddot{\phi}\zeta}\ _2$
Passive	0.0752	0.009	4.7347	2.1738	1.3562	3.9816
Problem 3.3	0.0746	0.0759	0.914	0.5664	0.562	0.4458

For the comparison purpose, the percentage changes of each suspension design

methodology over the passive one are shown in Table 3.5. The percentage changes are computed as follows:

$$\% \text{ change} = \frac{\|\cdot\|_{\text{passive}} - \|\cdot\|_{\text{controlled}}}{\|\cdot\|_{\text{passive}}} \times 100 \quad (3.15)$$

The results show that the design using Problem 3.1 provide a good compromises

Table 3.5. *The percentage changes of each active suspension design methodology over the passive one.*

% Change	$\ T_{r_1\zeta}\ _2$	$\ T_{r_2\zeta}\ _\infty$	$\ T_{r_3\zeta}\ _2$	$\ T_{\dot{z}_d\zeta}\ _2$	$\ T_{\dot{\theta}\zeta}\ _2$	$\ T_{\dot{\phi}\zeta}\ _2$
LQG	6.72%	1.29%	32.87%	37.18%	33.98%	31.52%
Problem 3.1	3.66%	18.28%	47.84%	39.46%	19.42%	55.26%
Problem 3.2	9.11%	-683.52%	74.62%	66.31%	49.51%	83.35%
Problem 3.3	0.83%	-739.92%	80.69%	73.94%	58.55%	88.8%

among the performance characteristics compared to other methodologies, where, it reduces RMS accelerations, the RMS suspension travels and the RMS tire deflections by 47.84%, 3.66% and 18.28%, respectively, in comparison with the passive one. The main drawbacks of the solutions of Problems 3.2 and 3.3 are deteriorating the RMS tire deflections by -683.52% and -739.92%, respectively.

4. SEMI ACTIVE SUSPENSION CONTROL DESIGN

In This chapter the classical semi active suspension controls namely skyhook, groundhook, and hybrid have been reviewed in Sections 4.2, 4.3 and 4.4, respectively. LMI optimization method has been proposed to obtain the semi active damping coefficients are presented in Section ???. Since the control designing is in discrete-time domain, a discretizing method discussed in Section 4.1.

4.1. Continuous Time System Discretization

As a previous step before discussing the semi active control methods, it is worth mentioning that the control designing in such these methods is in real time which involved a procedure for discretizing the continuous-time state space equations. The discrete-time state equation and output equation should be derived that yield the exact values at $t = kT$, where $k = 0, 1, 2, \dots$

Recall the continuous-time state and output equations 2.10 and 3.2:

$$\dot{x} = Ax + B_{\zeta}\zeta + B_u u$$

$$r = C_r x + D_{r\zeta}\zeta + D_{ru} u$$

The discrete-time representation of the equations 2.10 and 3.2 will take the form:

$$x((k+1)T) = A_d(T)x(kT) + B_{d\zeta}(T)\zeta(kT) + B_{du}(T)u(kT) \quad (4.1)$$

$$r(kT) = C_r x(kT) + D_{r\zeta}\zeta(kT) + D_{ru}u(kT) \quad (4.2)$$

where:

$$\begin{aligned}
A_d(T) &= e^{AT} \\
B_{d\zeta}(T) &= \left(\int_0^T e^{A\lambda} d\lambda \right) B_\zeta = A^{-1}(e^{AT} - I)B_\zeta \\
B_{du}(T) &= \left(\int_0^T e^{A\lambda} d\lambda \right) B_u = A^{-1}(e^{AT} - I)B_u
\end{aligned}$$

where A is nonsingular matrix. Since the sampling period T is fixed, the matrices A_d , $B_{d\zeta}$ and B_{du} are constant. The matrices C_r , $D_{r\zeta}$ and D_{ru} do not depend on the sampling period T . For detailed derivations see (Ogata et al., 1995).

4.2. Skyhook Approach

The principle of this approach is to design a controllers so that the vehicle body is “linked” to the sky frame in order to reduce the vertical oscillations of the chassis and the axle independently of each other (Savaresi et al., 2010). The skyhook configuration is shown in Fig.4.1 which the fictitious dampers c_{sky_i} link the sprung mass m_s to some inertial references in sky. The skyhook dampers focus on sprung mass to isolate it from road excitation, by increasing the skyhook damping coefficient the motion of the sprung mass decreases, so the skyhook control is considered as comfort oriented semi active control approach.

The equations of motion of this system are as follows:

Bouncing of the sprung mass:

$$\begin{aligned}
m_s \ddot{z}_G &= -k_1(z_1 - z_{u_1}) - k_2(z_2 - z_{u_2}) - k_3(z_3 - z_{u_3}) - k_4(z_4 - z_{u_4}) \\
&\quad - c_1(\dot{z}_1 - \dot{z}_{u_1}) - c_2(\dot{z}_2 - \dot{z}_{u_2}) - c_3(\dot{z}_3 - \dot{z}_{u_3}) - c_4(\dot{z}_4 - \dot{z}_{u_4}) \\
&\quad - F_{sky_1} - F_{sky_2} - F_{sky_3} - F_{sky_4} \quad (4.3)
\end{aligned}$$

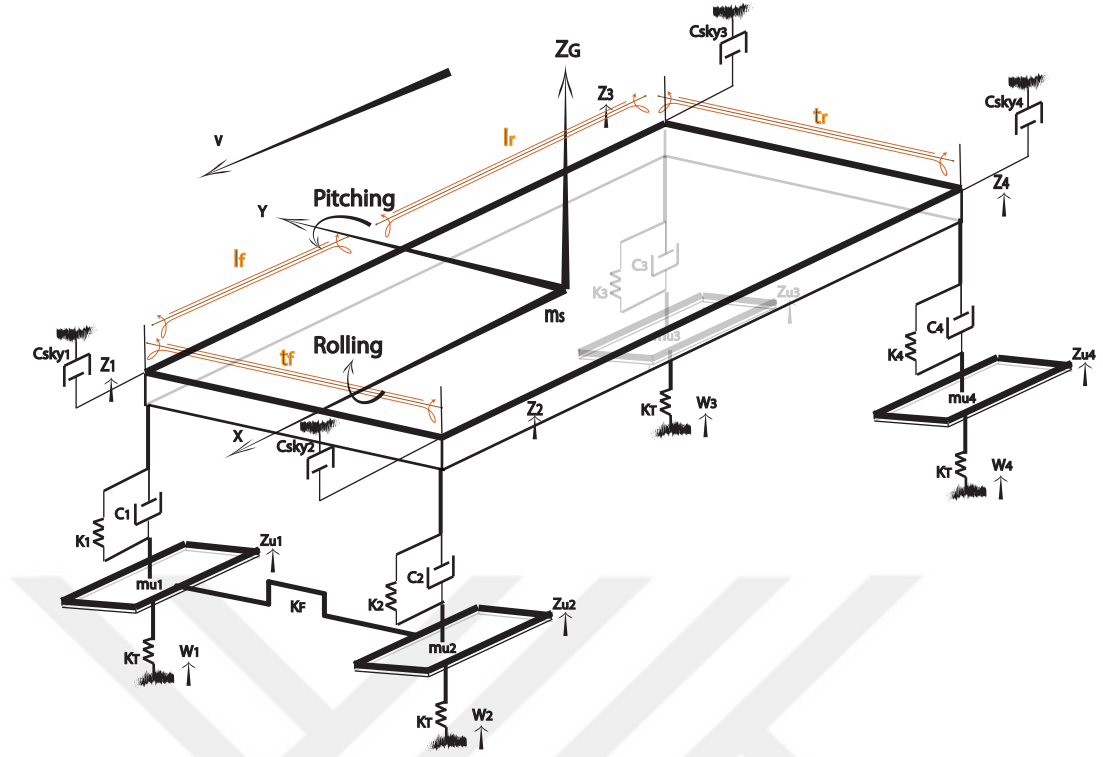


Figure 4.1. Ideal skyhook configuration of full car model.

Pitching of the sprung mass:

$$\begin{aligned}
 I_y \ddot{\theta} = & k_1 l_f (z_1 - z_{u1}) + k_2 l_f (z_2 - z_{u2}) - k_3 l_r (z_3 - z_{u3}) - k_4 l_r (z_4 - z_{u4}) \\
 & + c_1 l_f (\dot{z}_1 - \dot{z}_{u1}) + c_2 l_f (\dot{z}_2 - \dot{z}_{u2}) - c_3 l_r (\dot{z}_3 - \dot{z}_{u3}) - c_4 l_r (\dot{z}_4 - \dot{z}_{u4}) \\
 & + l_f F_{sky1} + l_f F_{sky2} - l_r F_{sky3} - l_r F_{sky4} \quad (4.4)
 \end{aligned}$$

Rolling of the sprung mass:

$$\begin{aligned}
 I_x \ddot{\phi} = & k_1 \frac{t_f}{2} (z_1 - z_{u1}) - k_2 \frac{t_f}{2} (z_2 - z_{u2}) + k_3 \frac{t_r}{2} (z_3 - z_{u3}) - k_4 \frac{t_r}{2} (z_4 - z_{u4}) \\
 & + c_1 \frac{t_f}{2} (\dot{z}_1 - \dot{z}_{u1}) - c_2 \frac{t_f}{2} (\dot{z}_2 - \dot{z}_{u2}) + c_3 \frac{t_r}{2} (\dot{z}_3 - \dot{z}_{u3}) - c_4 \frac{t_r}{2} (\dot{z}_4 - \dot{z}_{u4}) \\
 & + \frac{t_f}{2} F_{sky1} - \frac{t_f}{2} F_{sky2} + \frac{t_r}{2} F_{sky3} - \frac{t_r}{2} F_{sky4} \quad (4.5)
 \end{aligned}$$

Vertical Direction for each wheel:

$$m_{u_i} \ddot{z}_{u_i} = k_i (z_i - z_{u_i}) + c_i (\dot{z}_i - \dot{z}_{u_i}) - k_T (z_{u_i} - w_i), \quad i=1, \dots, 4 \quad (4.6)$$

where all the vehicle parameters and the variables are kept without change as in Chapter 2 except that the passive damping coefficients c_i are replaced by some smaller values defined later in this chapter and $F_{sky_i} = c_{sky_i} \dot{z}_i$ is the skyhook damping force with $c_{sky_i} > c_i$, $i = 1, \dots, 4$.

The frequency response of this system for different values of the skyhook damping coefficient c_{sky_i} are shown in Fig.4.2 and it can be noticed that as the skyhook damping coefficient increases the frequency response around the natural frequency of sprung mass ($\approx 10\text{rad/sec}$) decreases.

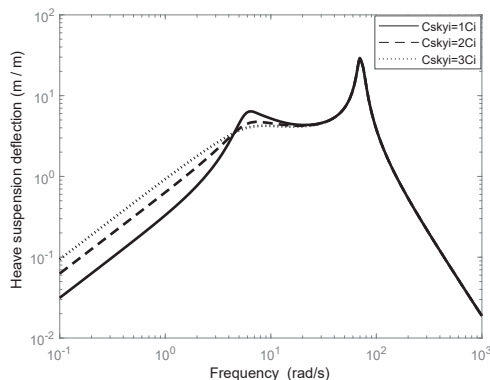


Figure 4.2. Heave suspension deflection frequency response for different values of c_{sky_i} .

But in realistic automotive applications the previous representation of skyhook control is not possible because the control elements should be between the sprung mass and the unsprung masses, so the alternative applicable skyhook control it will be discussed as follows.

The alternative configuration must be as showed in Fig.2.1 where a semi active dampers are mounted in parallel to passive suspension components. The main functionality of semi active dampers are to generate adjusted damping forces under different conditions on the sprung mass to imitate the ideal skyhook control performance. Once the semi active damper is chosen for realization, one must determine how to adjust the damper such that emulates the skyhook damper. First let us define some parameters and conventions that will be used throughout the controller designing. The parameters which induced by i is for $i = 1, 2, 3$ and 4 which refer to

the front-left, the front-right, the rear-left, and the rear-right corners of the vehicle, respectively. There is a relation between the c_{sky_i} and c_i such that $c_{sky_i} = c_{max_i} - c_{min_i}$, where $c_{min_i} = c_i$. The relative velocity is $(\dot{z}_i - \dot{z}_{u_i})$, and when the two masses (m_{u_i} and the part i of the sprung mass) are separating it means that $(\dot{z}_i - \dot{z}_{u_i})$ is positive, and when the two masses (m_{u_i} and the part i of the sprung mass) are coming together it means that $(\dot{z}_i - \dot{z}_{u_i})$ is negative. Now under these definitions, in the case when the part i of the sprung mass is moving upwards (\dot{z}_i is positive) and the two masses are separating then the ideal skyhook force due to skyhook damper c_{sky_i} is:

$$F_{sky_i} = -c_{max_i} \dot{z}_i \quad (4.7)$$

the semi active force due to semi active damper c_{sa_i} which is in tension is:

$$F_{sa_i} = -c_{sa_i} (\dot{z}_i - \dot{z}_{u_i}) \quad (4.8)$$

to emulate the skyhook damper the semi active damper should generate force equal to the force generated by the skyhook damper, or:

$$F_{sky_i} = -c_{max_i} \dot{z}_i = -c_{sa_i} (\dot{z}_i - \dot{z}_{u_i}) = F_{sa_i} \quad (4.9)$$

by solving for c_{sa_i} in terms of c_{max_i} and using the solution to find the semi active damping force:

$$c_{sa_i} = \frac{c_{max_i}}{(\dot{z}_i - \dot{z}_{u_i})} \dot{z}_i \Rightarrow F_{sa_i} = c_{max_i} \dot{z}_i \quad (4.10)$$

in the case when the part i of the sprung mass is moving downwards (\dot{z}_i is negative) and the two masses are coming together then the ideal skyhook force due to skyhook damper c_{sky_i} is:

$$F_{sky_i} = c_{max_i} \dot{z}_i \quad (4.11)$$

the semi active force due to semi active damper c_{sa_i} which is in compression is:

$$F_{sa_i} = c_{sa_i}(\dot{z}_i - \dot{z}_{u_i}) \quad (4.12)$$

to emulate the skyhook damper the semi active damper should generate force equal to the force generated by the skyhook damper, or:

$$F_{sky_i} = c_{max_i} \dot{z}_i = c_{sa_i}(\dot{z}_i - \dot{z}_{u_i}) = F_{sa_i} \quad (4.13)$$

by solving for c_{sa_i} in terms of c_{max_i} and using the solution to find the semi active damping force:

$$c_{sa_i} = \frac{c_{max_i}}{(\dot{z}_i - \dot{z}_{u_i})} \dot{z}_i \Rightarrow F_{sa_i} = c_{max_i} \dot{z}_i \quad (4.14)$$

It can be conclude that when the product $\dot{z}_i(\dot{z}_i - \dot{z}_{u_i})$ is positive then the semi active damping force is defined by Eq.4.14. In the case when the part i of the sprung mass is moving upwards (\dot{z}_i is positive) and the two masses are coming together then the ideal skyhook force due to skyhook damper c_{sky_i} is in the negative direction, the semi active damper c_{sa_i} which is in compression can not apply force in the same direction as the skyhook damper, so in this case minimum damping is preferred to be applied by the semi active damper. The final case, when the part i of the sprung mass is moving downwards (\dot{z}_i is negative) and the two masses are separating then the ideal skyhook force due to skyhook damper c_{sky_i} is in the positive direction, the semi active damper c_{sa_i} which is in tension can not apply force in the same direction as the skyhook damper, so in this case minimum damping is preferred to be applied by the semi active damper. Summarizing these four cases, the well known skyhook policy (Goncalves, 2001) can be written as follows:

$$F_{sa_i} = \begin{cases} c_{max_i} \dot{z}_i & \text{if } \dot{z}_i(\dot{z}_i - \dot{z}_{u_i}) \geq 0 \\ 0 & \text{if } \dot{z}_i(\dot{z}_i - \dot{z}_{u_i}) < 0 \end{cases} \quad (4.15)$$

Substituting the semi active damping force $F_{sai} = u_i$ to the Equations 2.1-2.4 the practical skyhook controlled semi active suspension system can be obtained.

4.3. Groundhook Approach

In a dual way to the skyhook case, now the fictitious dampers c_{gro_i} link the unsprung masses m_{u_i} to some inertial references in ground. The groundhook configuration is shown in Fig.4.3. The groundhook dampers focus on unsprung masses to keep them

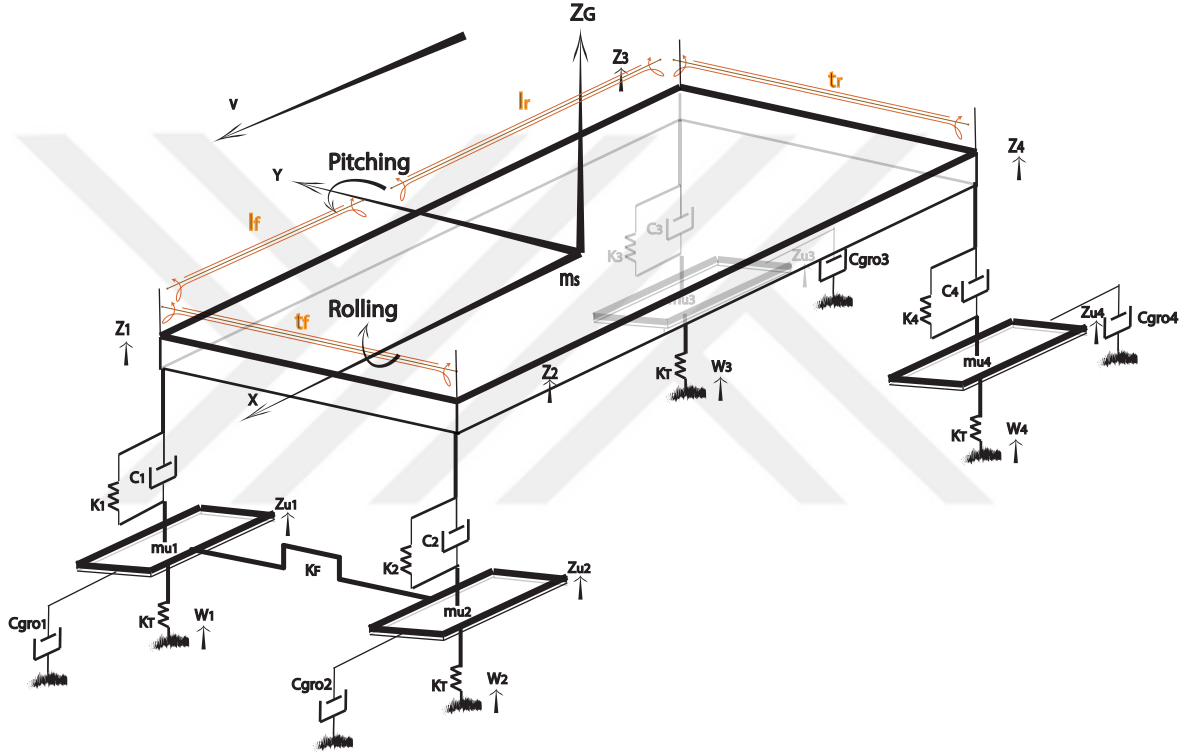


Figure 4.3. Ideal groundhook configuration of full car model.

in constant contact with road surface as possible, by increasing the groundhook damping coefficients the motion of the unsprung masses decreases, so the groundhook control is considered as road holding oriented semi active control approach.

The equations of motion of this system are as follows:

Bouncing of the sprung mass:

$$m_s \ddot{z}_G = -k_1(z_1 - z_{u1}) - k_2(z_2 - z_{u2}) - k_3(z_3 - z_{u3}) - k_4(z_4 - z_{u4}) - c_1(\dot{z}_1 - \dot{z}_{u1}) - c_2(\dot{z}_2 - \dot{z}_{u2}) - c_3(\dot{z}_3 - \dot{z}_{u3}) - c_4(\dot{z}_4 - \dot{z}_{u4}) \quad (4.16)$$

Pitching of the sprung mass:

$$I_y \ddot{\theta} = k_1 l_f (z_1 - z_{u_1}) + k_2 l_f (z_2 - z_{u_2}) - k_3 l_r (z_3 - z_{u_3}) - k_4 l_r (z_4 - z_{u_4}) \\ + c_1 l_f (\dot{z}_1 - \dot{z}_{u_1}) + c_2 l_f (\dot{z}_2 - \dot{z}_{u_2}) - c_3 l_r (\dot{z}_3 - \dot{z}_{u_3}) - c_4 l_r (\dot{z}_4 - \dot{z}_{u_4}) \quad (4.17)$$

Rolling of the sprung mass:

$$I_x \ddot{\phi} = k_1 \frac{t_f}{2} (z_1 - z_{u_1}) - k_2 \frac{t_f}{2} (z_2 - z_{u_2}) + k_3 \frac{t_r}{2} (z_3 - z_{u_3}) - k_4 \frac{t_r}{2} (z_4 - z_{u_4}) \\ + c_1 \frac{t_f}{2} (\dot{z}_1 - \dot{z}_{u_1}) - c_2 \frac{t_f}{2} (\dot{z}_2 - \dot{z}_{u_2}) + c_3 \frac{t_r}{2} (\dot{z}_3 - \dot{z}_{u_3}) - c_4 \frac{t_r}{2} (\dot{z}_4 - \dot{z}_{u_4}) \quad (4.18)$$

Vertical Direction for each wheel:

$$m_{u_i} \ddot{z}_{u_i} = k_i (z_i - z_{u_i}) + c_i (\dot{z}_i - \dot{z}_{u_i}) - k_T (z_{u_i} - w_i) - F_{gro_i}, \quad i=1, \dots, 4 \quad (4.19)$$

where all the vehicle parameters and the variables are kept without change as in Chapter 2 except that the passive damping coefficients c_i are replaced by some smaller values defined later in this chapter and $F_{gro_i} = c_{gro_i} \dot{z}_{u_i}$ is the groundhook damping force with $c_{gro_i} > c_i$, $i = 1, \dots, 4$.

The frequency response of this system for different values of the groundhook damping coefficients c_{gro_i} are shown in Fig.4.4 and it can be noticed that as the groundhook damping coefficient increases the frequency response around the natural frequency of unsprung mass ($\approx 100 \text{ rad/sec}$) decreases.

But in realistic automotive applications the previous representation of groundhook control is not possible. The alternative configuration must be as showed in Fig.2.1 where a semi active dampers are mounted in parallel to passive suspension components. The main functionality of semi active dampers are to generate adjusted damping forces under different conditions on the unsprung mass to imitate the ideal groundhook control performance. Once the semi active damper is chosen for realization, one must determine how to adjust the damper such that emulates

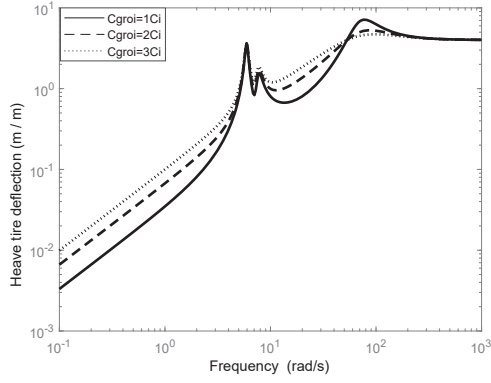


Figure 4.4. Heave tire deflection frequency response for different values of $c_{gro_i}s$.

the groundhook damper. As in skyhook case there is a relation between the c_{gro_i} and c_i such that $c_{gro_i} = c_{max_i} - c_{min_i}$, where $c_{min_i} = c_i$. The well known groundhook control policy can be derived through the same reasoning used for skyhook control (Goncalves, 2001):

$$F_{sai} = \begin{cases} c_{max_i} \dot{z}_{u_i} & \text{if } -\dot{z}_{u_i}(\dot{z}_i - \dot{z}_{u_i}) \geq 0 \\ 0 & \text{if } -\dot{z}_{u_i}(\dot{z}_i - \dot{z}_{u_i}) < 0 \end{cases} \quad (4.20)$$

Substituting the semi active damping force $F_{sai} = u_i$ to the Equations 2.1-2.4 the groundhook controlled semi active suspension system can be derived.

4.4. Hybrid Approach

An alternative semi active control policy known as hybrid control has been shown to take advantage of the benefits of both skyhook and groundhook control (Goncalves, 2001). The suspension system with hybrid control can be set up to operate as skyhook or groundhook controlled system, or a combination of both. The hybrid configuration is shown in Fig.4.5.

The equations of motion of this system are as follows:

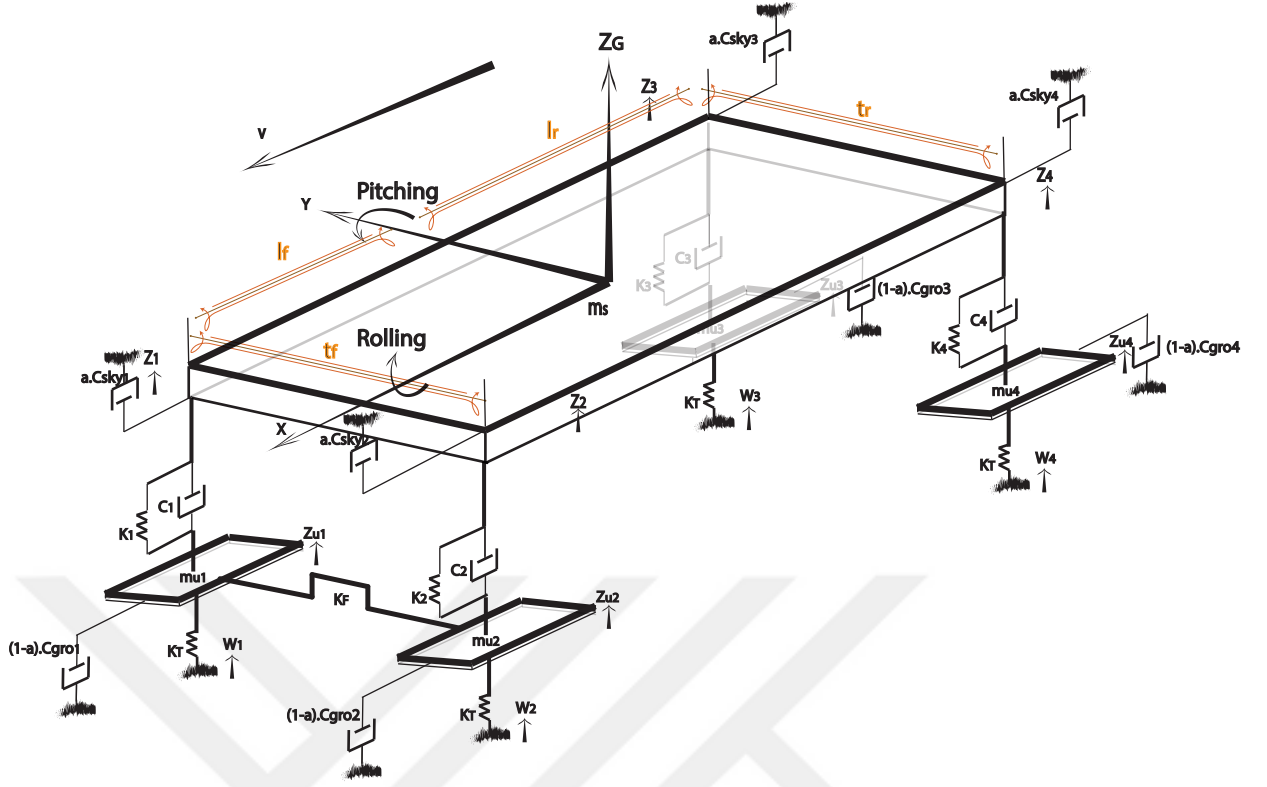


Figure 4.5. Ideal hybrid configuration of full car model.

Bouncing of the sprung mass:

$$\begin{aligned}
 m_s \ddot{z}_G = & -k_1(z_1 - z_{u1}) - k_2(z_2 - z_{u2}) - k_3(z_3 - z_{u3}) - k_4(z_4 - z_{u4}) \\
 & - c_1(\dot{z}_1 - \dot{z}_{u1}) - c_2(\dot{z}_2 - \dot{z}_{u2}) - c_3(\dot{z}_3 - \dot{z}_{u3}) - c_4(\dot{z}_4 - \dot{z}_{u4}) \\
 & - \alpha_1 F_{sky1} - \alpha_2 F_{sky2} - \alpha_3 F_{sky3} - \alpha_4 F_{sky4} \quad (4.21)
 \end{aligned}$$

Pitching of the sprung mass:

$$\begin{aligned}
 I_y \ddot{\phi} = & k_1 l_f(z_1 - z_{u1}) + k_2 l_f(z_2 - z_{u2}) - k_3 l_r(z_3 - z_{u3}) - k_4 l_r(z_4 - z_{u4}) \\
 & + c_1 l_f(\dot{z}_1 - \dot{z}_{u1}) + c_2 l_f(\dot{z}_2 - \dot{z}_{u2}) - c_3 l_r(\dot{z}_3 - \dot{z}_{u3}) - c_4 l_r(\dot{z}_4 - \dot{z}_{u4}) \\
 & + l_f \alpha_1 F_{sky1} + l_f \alpha_2 F_{sky2} - l_r \alpha_3 F_{sky3} - l_r \alpha_4 F_{sky4} \quad (4.22)
 \end{aligned}$$

Rolling of the sprung mass:

$$\begin{aligned}
I_x \ddot{\theta} = & k_1 \frac{t_f}{2} (z_1 - z_{u_1}) - k_2 \frac{t_f}{2} (z_2 - z_{u_2}) + k_3 \frac{t_r}{2} (z_3 - z_{u_3}) - k_4 \frac{t_r}{2} (z_4 - z_{u_4}) \\
& + c_1 \frac{t_f}{2} (\dot{z}_1 - \dot{z}_{u_1}) - c_2 \frac{t_f}{2} (\dot{z}_2 - \dot{z}_{u_2}) + c_3 \frac{t_r}{2} (\dot{z}_3 - \dot{z}_{u_3}) - c_4 \frac{t_r}{2} (\dot{z}_4 - \dot{z}_{u_4}) \\
& + \frac{t_f}{2} \alpha_1 F_{sky_1} - \frac{t_f}{2} \alpha_2 F_{sky_2} + \frac{t_r}{2} \alpha_3 F_{sky_3} - \frac{t_r}{2} \alpha_4 F_{sky_4} \quad (4.23)
\end{aligned}$$

Vertical Direction for each wheel:

$$m_{u_i} \ddot{z}_{u_i} = k_i (z_i - z_{u_i}) + c_i (\dot{z}_i - \dot{z}_{u_i}) - K_T (z_{u_i} - w_i) - (1 - \alpha_i) F_{gro_i}, \quad i=1, \dots, 4 \quad (4.24)$$

where all the vehicle parameters and the variables are kept without change as in Chapter 2 except that the passive damping coefficients c_i are replaced by some smaller values defined later in this chapter. $F_{gro_i} = c_{gro_i} \dot{z}_{u_i}$ is the groundhook damping force with $c_{gro_i} > c_i$, $F_{sky_i} = c_{sky_i} \dot{z}_i$ is the skyhook damping force with $c_{sky_i} > c_i$ and α_i is the relative ratio between the skyhook and groundhook control for $i = 1, 2, 3$ and 4.

From these equations it can be noticed that, when α_i is 0 the system is reduced to be groundhook controlled suspension system, and when α_i is 1 the system is reduced to be skyhook controlled suspension system. The frequency responses in the figures 4.6 and 4.7 show that the value 0.5 of α_i yields a good trade-off between skyhook and groundhook controlled suspension systems.

But in realistic automotive applications the previous representation of hybrid control is not possible. The alternative configuration must be as showed in Fig.2.1. Combining the equations 4.15 and 4.20 the well known hybrid control policy can be derived:

$$\sigma_{gro_i} = \begin{cases} \dot{z}_{u_i} & \text{if } -\dot{z}_{u_i} (\dot{z}_i - \dot{z}_{u_i}) \geq 0 \\ 0 & \text{if } -\dot{z}_{u_i} (\dot{z}_i - \dot{z}_{u_i}) < 0 \end{cases}$$

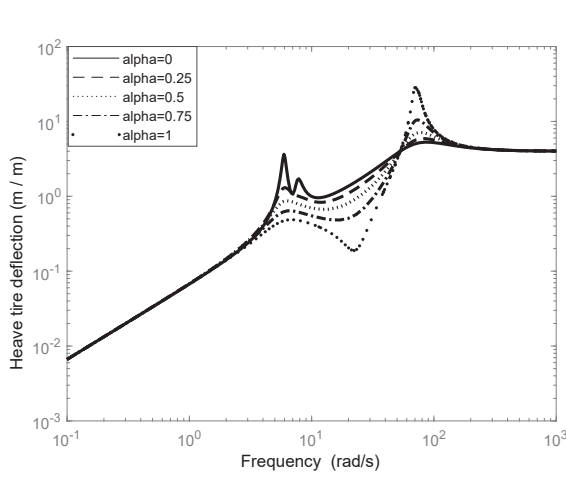


Figure 4.6. Heave tire deflection frequency response for different values of α_i s for $c_{sky_i} = c_{gro_i} = 2c_i$.

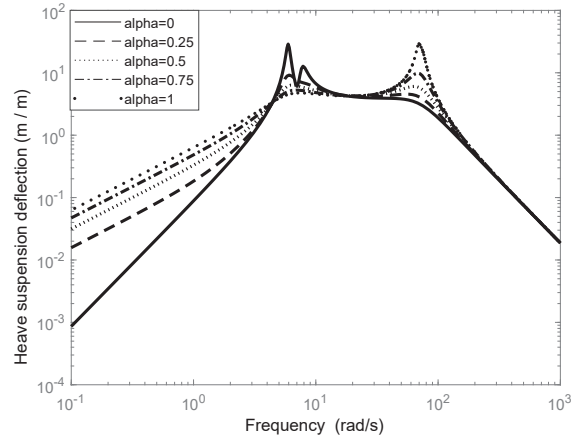


Figure 4.7. Heave suspension deflection frequency response for different values of α_i s for $c_{sky_i} = c_{gro_i} = 2c_i$.

$$\sigma_{sky_i} = \begin{cases} \dot{z}_i & \text{if } \dot{z}_i(\dot{z}_i - \dot{z}_{u_i}) \geq 0 \\ 0 & \text{if } \dot{z}_i(\dot{z}_i - \dot{z}_{u_i}) < 0 \end{cases}$$

then the hybrid control law is:

$$F_{sa_i} = G_i(\alpha_i \sigma_{sky_i} + (1 - \alpha_i) \sigma_{gro_i}) \quad (4.25)$$

where G_i is a constant gain and equals c_{max_i} . Substituting the semi active damping force $F_{sa_i} = u_i$ to the Equations 2.1-2.4 the hybrid controlled semi active suspension system can be derived.

The design parameters for the three approaches are chosen as follows (Blanchard, 2003):

$$c_{min_i} = 0.2c_i \text{ and } c_{max_i} = 2.2c_i \quad (4.26)$$

where c_i are the passive damping coefficients as defined in Table 2.1, and in the configuration Figs 4.1, 4.3 and 4.5 c_i are c_{min_i} instead, $i = 1, \dots, 4$.

The frequency responses of the skyhook, groundhook and hybrid controlled suspension to roll input ($\zeta_1 = -\zeta_2 = \zeta_3 = -\zeta_4$) compared to passive one were ex-

amined and shown in Figs 4.8 -4.10. From frequency response figures it can be

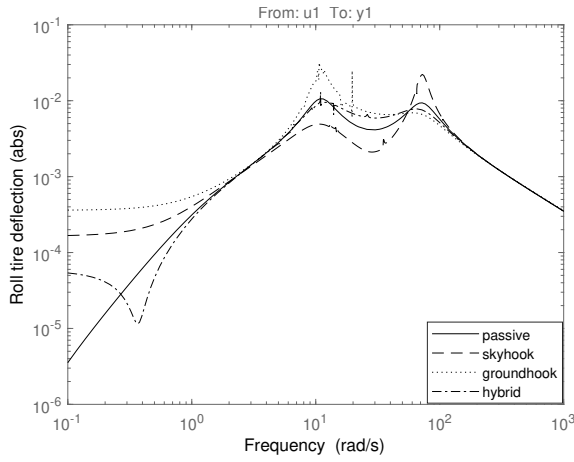


Figure 4.8. Roll tire deflection frequency response to roll input.

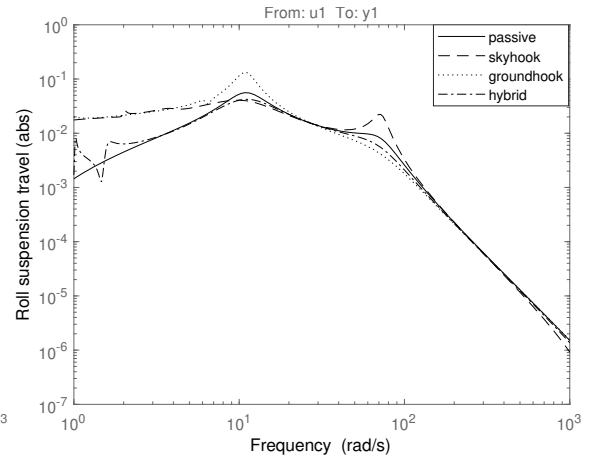


Figure 4.9. Roll suspension travel frequency response to roll input.

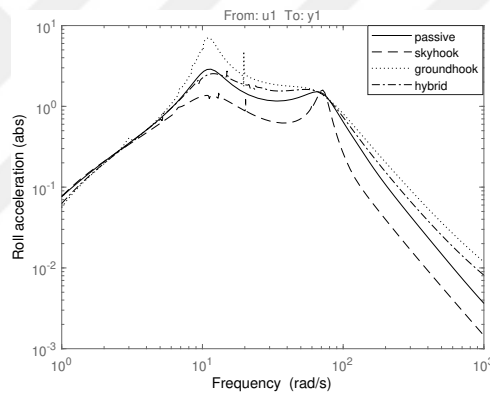


Figure 4.10. Roll acceleration frequency response to roll input.

concluded that skyhook control improves the response at low frequencies (around the sprung mass natural frequency), while increases the response at high frequencies (around the unsprung mass natural frequency), that means the skyhook control successes in improving ride comfort performance but fails in improving road holding performance. Otherwise, groundhook control improves the response at high frequencies (around the unsprung mass natural frequency), while increases the response at low frequencies (around the sprung mass natural frequency), that means the groundhook control successes in improving road holding performance but fails in improving ride comfort performance which it is worse than passive suspension. Hybrid control provides a good compromise between skyhook and groundhook controls, such that

improves ride comfort and road holding at the same time and still performs somehow better than the passive suspension system.



5. LMI OPTIMIZATION OF SKYHOOK CONTROL

In literature specially in (Blanchard, 2003), (Ihsan et al., 2008) and (Du et al., 2005) works, they have not presented a methodical way to find the design parameters (c_{min_i} , c_{max_i}) of skyhook control law. In (Poussot-Vassal et al., 2006) an optimization method has been proposed but for a quarter car model. Here, a novel methodology based on LMI optimization is proposed and introduced to upgrade the aforementioned design parameters.

5.1. Conventional Skyhook Control Law

For the design of a feedback law for skyhook control which discussed in Section 4.2, consider the measurements of the vertical velocity at each corner of the sprung mass and the suspension velocities, which can be written as:

$$y = C_y x \tag{5.1}$$

where:

$$y = \begin{pmatrix} \dot{z}_1 \dots \dot{z}_4 & \dot{z}_1 - \dot{z}_{u1} \dots \dot{z}_4 - \dot{z}_{u4} \end{pmatrix}$$

$$C_y = \begin{pmatrix} 0_{4 \times 7} & \Psi & 0_{4 \times 4} & 0_{4 \times 4} \\ 0_{4 \times 7} & \Psi & -I_4 & 0_{4 \times 4} \end{pmatrix}$$

The static output feedback structure is:

$$u(k) = Fy(k) \tag{5.2}$$

where the gain F is to be determined in this section. It is worth mentioning that the skyhook controller F designing is in discrete time domain, so the system is discretized as discussed in Section 4.1 for sampling time $T = 10^{-2} \text{ sec}$. In order to find F the following theorems are reviewed.

Theorem 5.1 (Discrete-time H_∞ state feedback): (De Oliveira et al., 2002)

There exists a controller in the form 5.2 such that the inequality $\|T_{r\zeta}(z)\|_\infty \leq \gamma_1^2$ holds if and only if the LMI

$$\begin{pmatrix} P & A_d X + B_{du} L & B_{d\zeta} & 0 \\ * & X + X^T - P & 0 & (C_r X + D_{ru} L)^T \\ * & * & I & D_{r\zeta}^T \\ * & * & * & \gamma_1 I \end{pmatrix} > 0$$

holds, where the matrices X and L and the symmetric matrix P are the variables of appropriate dimensions.

Theorem 5.2 (Discrete-time H_2 state feedback): (De Oliveira et al., 2002)

There exists a controller in the form 5.2 such that the inequality $\|T_{r\zeta}(z)\|_2 \leq \gamma_2^2$ holds if and only if the LMIs

$$\begin{pmatrix} P & A_d X + B_{du} L & B_{d\zeta} \\ * & X + X^T - P & 0 \\ * & * & I \end{pmatrix} > 0,$$

$$\begin{pmatrix} W & C_r X + D_{ru} L \\ * & X + X^T - P \end{pmatrix} > 0 \text{ and}$$

$$\text{Trace}(W) < \gamma_2$$

hold, where the matrices X and L and the symmetric matrices P and W are the variables of appropriate dimensions.

It is desired to synthesize static output feedback problem. In order to solve static output feedback problems involving stability and multi-objective control it is assumed that the measurement matrix C_y in 5.1 could be transformed to the form

[I 0] see Remark 5.1, and the LMI variables L and X should have the structures:

$$L := \begin{pmatrix} L_{out} & 0 \end{pmatrix}, X := \begin{pmatrix} X_{out} & 0 \\ X_{12} & X_{22} \end{pmatrix} \quad (5.3)$$

Then a static output feedback gain F is found in form 5.2, where in the context of state feedback problem:

$$K = \begin{pmatrix} F & 0 \end{pmatrix} = \begin{pmatrix} L_{out} X_{out}^{-1} & 0 \end{pmatrix} \quad (5.4)$$

where K is the state feedback gain.

For the skyhook control problem the measurements $(\dot{z}_1 \dots \dot{z}_4)$ are needed to the feedback, while the others $(\dot{z}_1 - \dot{z}_{u_1} \dots \dot{z}_4 - \dot{z}_{u_4})$ are needed to formulate the actuating conditions in 4.15. Each input u_i is allowed to get feedback only from the corresponding measurement y_i , this leads to adopt the decentralized control concept (Rubió-Massegú et al., 2013). In order to solve this issue, a diagonal structure is imposed on the matrices L_{out} and X_{out} to derive a diagonal matrix for the gain F .

Remark 5.1 *The measurement matrix C_y in 5.1 shall be full row ranked to be able to be transformed to [I 0] but it is not. To overcome this problem the following remedy is suggested: Since the forth row \dot{z}_4 is linearly dependent on the first three rows, it can be written with respect to them as:*

$$\dot{z}_4 = -\frac{t_r}{t_f} \dot{z}_1 + \frac{t_r}{t_f} \dot{z}_2 + \dot{z}_3$$

so it can be omitted provided that the skyhook damping coefficients at the rear corners c_{sky_3} and c_{sky_4} are equal. Then, the measuring signals are reduced to 7 instead of 8. A similarity transformation matrix T_{tr} generally is not unique. A special form can be obtained by:

$$T_{tr} = \begin{pmatrix} C_y^T (C_y C_y^T)^{-1} & C_y^\perp \end{pmatrix}$$

where C_y^\perp denotes an orthogonal basis for the null space of C_y .

Recall the Problem 3.1 but in discrete time domain which can be reformulated as follows:

Problem 5.1 Given H_∞ norm bound γ_1 design a static output feedback controller with gain F that minimizes

$$\beta_1 \|T_{r_1\zeta}(z)\|_2 + \beta_2 \|T_{r_3\zeta}(z)\|_2$$

subject to $\|T_{r_2\zeta}(z)\|_\infty \leq \gamma_1$.

Employing the Theorems 5.1 and 5.2 for the **ideal** skyhook system 4.3-4.6 (without changing the passive damping coefficients) and the measurement equation 5.1 taking into account the aforementioned discussions and Remark 5.1 the solution for the controller gain F is found:

$$F = \left(\text{diag}(4978.3, 4978.3, 511.1, 511.1) \quad 0_{4 \times 4} \right) \quad (5.5)$$

Thus,

$$c_{sky_i} = 4978.3, \quad i = 1, 2 \quad (5.6)$$

$$c_{sky_i} = 511.1, \quad i = 3, 4 \quad (5.7)$$

In Section 4.2 it has been clarified that the **ideal** skyhook configuration is not feasible and the alternative **practical** one that handling actuating conditions has been proposed for the realization of skyhook concept. The damping coefficient of the semi active dampers have the relation with the skyhook ones:

$$c_{max_i} = c_{sky_i} + c_{min_i} = 4978.3 + 0.2c_i = 4.059c_i, \quad i = 1, 2 \quad (5.8)$$

$$c_{max_i} = c_{sky_i} + c_{min_i} = 511.1 + 0.2c_i = 0.515c_i, \quad i = 3, 4 \quad (5.9)$$

where c_i the passive damping coefficients defined in the Table 2.1. In skyhook policy 4.15 the minimal damping coefficients are $c_{min_i} = 0.2c_i$ instead of zeros. Moreover, after applying several simulations on different values of the passive damping coefficients, it is found that the modified values $c_i = 0.2c_i$ give the best results.

After synthesizing the *practical* skyhook suspension with the upgraded maximal and minimum damping coefficients c_{max_i} and c_{min_i} , respectively, the stochastic responses of the skyhook suspension with the obtained design parameters are computed as follows:

$$RMS(r_i) = \sqrt{\frac{1}{N} \sum_{n=1}^N |r_{i_n}|^2} \quad (5.10)$$

where N is number of samples and r_i is the regulated output for $i = 1, \dots, 11$. The results are compared to skyhook suspension design in (Blanchard, 2003) and displayed in Table 5.1. The results show the advantages of keeping some passive

Table 5.1. *The stochastic responses of the passive and Conventional skyhook suspensions.*

RMS	(Blanchard, 2003)		
	Passive	Skyhook Configuration	LMI Conventional Skyhook
Heave-Suspension Travels	0.0046	0.0071	0.0049
Benefit vs passive	-	-55.2%	-6.27%
Heave-Tire deflections	0.0016	0.0056	0.0024
Benefit vs passive	-	-252.64%	-49.41%
Heave Acceleration	0.1522	0.13	0.1008
Benefit vs passive	-	11.65%	33.78%
Pitch Acceleration	0.0935	0.07	0.0630
Benefit vs passive	-	24.69%	32.59%
Roll Acceleration	0.28	0.2591	0.186
Benefit vs passive	-	7.47%	33.28%

damping forces accompanying the semi active damping forces while synthesizing the skyhook controller, because in some works in literature like (Blanchard, 2003) the passive dampers are excluded from the suspension system. However, the suspension travels and tire deflections performances are deteriorated compared to passive suspension and this problem leads to consider more powerful alternative skyhook

control law to overcome these drawbacks.

5.2. Alternative Skyhook Control Law

The conventional semi active damper that proposed in the previous section can only generate the damping force proportional to body's corner velocity (\dot{z}_i) which results in worse responses with respect to drive safety as seen in Table 5.1. An alternative version of skyhook control law has been utilized to conduct a variable damping as clarified in (Sammier et al., 2003) and (Poussot-Vassal et al., 2006). In this version of skyhook control the body's corner vertical velocity (\dot{z}_i) as well as the axle velocity (\dot{z}_{ui}) affect the body and axle accelerations. Unlike to conventional skyhook control in which the body and axle accelerations are merely affected by the body's corner vertical velocity (\dot{z}_i). The adapted semi active damper that emulates a skyhook damper consists in changing the damping coefficient according to the body's corner vertical speed (\dot{z}_i) and to the suspension deflection speed ($\dot{z}_i - \dot{z}_{ui}$) such that generates the damping force as follows:

$$u_i = \begin{cases} \alpha c_{max_i}(\dot{z}_i - \dot{z}_{u_i}) + (1 - \alpha)c_{max_i}\dot{z}_i & \text{if } \dot{z}_i(\dot{z}_i - \dot{z}_{u_i}) \geq 0 \\ c_{min_i}(\dot{z}_i - \dot{z}_{u_i}) & \text{if } \dot{z}_i(\dot{z}_i - \dot{z}_{u_i}) < 0 \end{cases} \quad (5.11)$$

where c_{max_i} and c_{min_i} are the maximal and minimal damping coefficients, respectively, achieved by the continuously variable controlled semi active damper (i.e. MR damper). $\alpha \in [0, 1]$ is a tuning parameter that modifies the suspension system behavior.

To design the control law in the on-mode in Eq. 5.11 the simplification made to ease the design procedure such that:

$$u_i = \alpha c_{max_i}(\dot{z}_i - \dot{z}_{u_i}) + (1 - \alpha)c_{max_i}\dot{z}_i \quad (5.12)$$

$$= c_{max_i}\dot{z}_i - \alpha c_{max_i}\dot{z}_{u_i} \quad (5.13)$$

Dealing with the control law in Eq.5.13 the measurements of body's corner vertical speeds (\dot{z}_i) and axle speeds (\dot{z}_{u_i}) are needed (which are usually not measurable in industrial application, but can be obtained by doing some numerical derivations and integrations on the measurable quantities). Modifying the measurements in Eq.5.1 the new ones can be written as:

$$y = C_y x \quad (5.14)$$

where:

$$y = \begin{pmatrix} \dot{z}_1 \dots \dot{z}_4 & \dot{z}_{u_1} \dots \dot{z}_{u_4} \end{pmatrix}$$

$$C_y = \begin{pmatrix} 0_{4 \times 7} & \Psi & 0_{4 \times 4} & 0_{4 \times 4} \\ 0_{4 \times 7} & 0_{4 \times 3} & I_4 & 0_{4 \times 4} \end{pmatrix}$$

Since the measurement matrix C_y is not full row rank, the Remark 5.1 should be taken into account to solve the Problem 5.1, except that the assumption on the damping coefficients to be equal at front side and at rear side is left out.

The gain F is desirable to take the form:

$$F = \left(\text{diag}(c_{max_1} \ c_{max_2} \ c_{max_3} \ c_{max_4}) \ -\alpha \times \text{diag}(c_{max_1} \ c_{max_2} \ c_{max_3} \ c_{max_4}) \right)$$

and this involves to impose a structural constraints on the LMI variables L and X as illustrated in 5.3 where:

$$L_{out} = \left(\left[\text{diag}(L_{out_1} \ L_{out_2} \ L_{out_3}) ; 0_{1 \times 3} \right] \ -\alpha \times \text{diag}(L_{out_1} \ L_{out_2} \ L_{out_3} \ L_{out_4}) \right)$$

$$X_{out} = \left(\text{diag}(X_{out_1} \ X_{out_2} \ X_{out_3} \ X_{out_4}) \ \text{diag}(X_{out_1} \ X_{out_2} \ X_{out_3} \ X_{out_4}) \right)$$

Employing the Theorems 5.1 and 5.2 for the discrete time suspension system 4.1-4.2 (without passive dampers) and the measurement equation 5.14 the solution for the controller gain F is found with fixed $\alpha = 0.5$ for the control law in Eq. 5.13:

$$c_{max_1} = 1759.6, \ c_{max_2} = 2059.3, \ c_{max_3} = 1065.9 \ \text{and} \ c_{max_4} = 1291.45 \quad (5.15)$$

For the realization of *practical* semi active suspension which handling the actuating condition on the semi active damper, the obtained design parameters 5.15 are synthesized to generate the damping force that illustrated in 5.11. The acceptable results are found by setting $c_{min_i} = 0.5c_i$ in 5.11 and passive damping coefficients $c_i = 0$. The relationship between the RMS performance quantities of the achieved suspension system and α are shown in Figs 5.1-5.5. In the range $\alpha < 0.5$ the RMS of heave, pitch and roll accelerations are less than their counterparts in the range $\alpha > 0.5$ which achieved ride comfort but at the expense of drive safety resulting in soft suspension. Furthermore, In the range $\alpha > 0.5$ the RMS of heave suspension travel and heave tire deflection are less than their counterparts in $\alpha < 0.5$ which achieved drive safety but at the expense of ride comfort resulting in hard suspension. The value

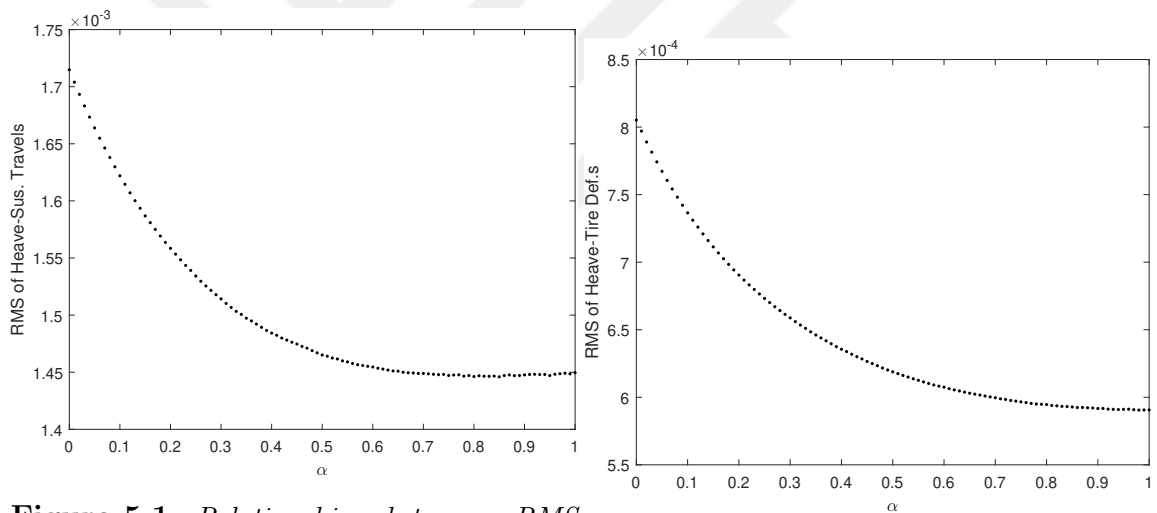


Figure 5.1. Relationship between RMS heave suspension travel and α . **Figure 5.2.** Relationship between RMS heave tire deflection and α .

0.5 of α gives a good compromise between the two conflicting objectives namely, the comfort ride and drive safety. The RMS values of the suspension responses are shown in Table 5.2 and the percentage change over the passive suspension also exhibited. The alternative control law 5.11 gives better results with respect to drive safety compared to the conventional one in 4.15.

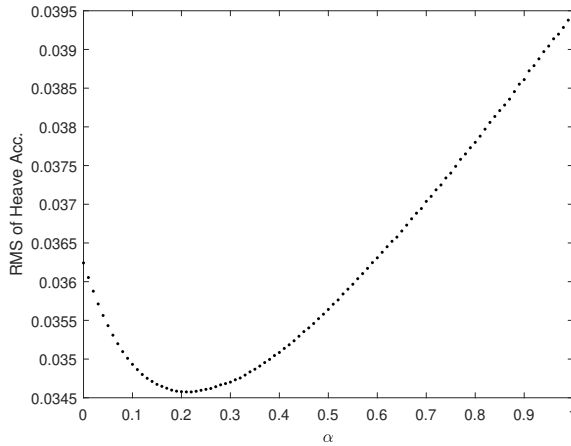


Figure 5.3. Relationship between RMS heave acceleration and α .

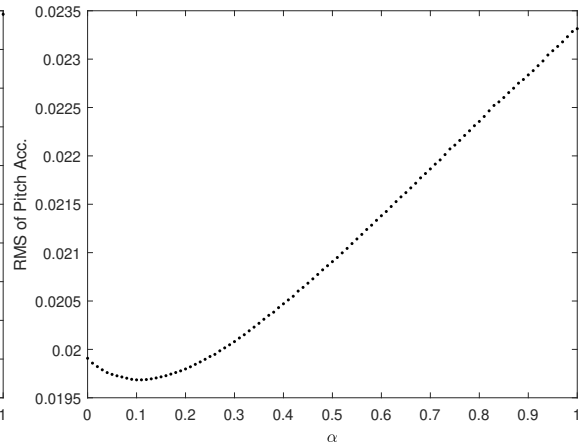


Figure 5.4. Relationship between RMS pitch acceleration and α .

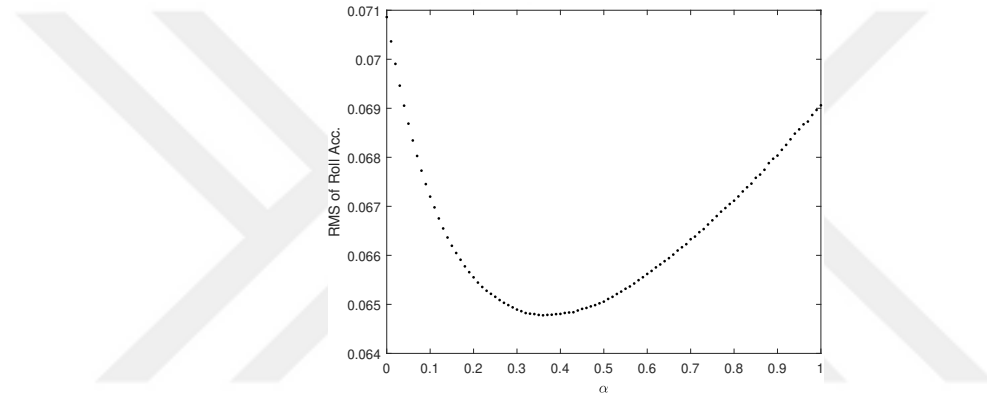


Figure 5.5. Relationship between RMS roll acceleration and α .

5.3. Frequency Domain Responses

For comparison purpose, the frequency responses for passive, active designed by solving Problem 3.1, and semi active designed by optimizing the alternative Skyhook suspension systems to roll input are plotted in Figures 5.6, 5.7 and 5.8 in order to understand how every frequency component affects the performance indices. Since the Skyhook control design is in real time, the transfer function of Skyhook controlled suspension system is estimated by the Matlab function `tfest`. The results show that how the semi active suspension is a compromise solution between the active and passive suspensions.

Table 5.2. *The stochastic responses of the passive and alternative skyhook suspension for $\alpha = 0.5$.*

RMS	LMI Alternative Skyhook
Heave-Suspension Travels Benefit vs passive	0.004 11.8%
Heave-Tire deflections Benefit vs passive	0.0017 -8%
Heave Acceleration Benefit vs passive	0.11 22%
Pitch Acceleration Benefit vs passive	0.07 24%
Roll Acceleration Benefit vs passive	0.21 24.9%

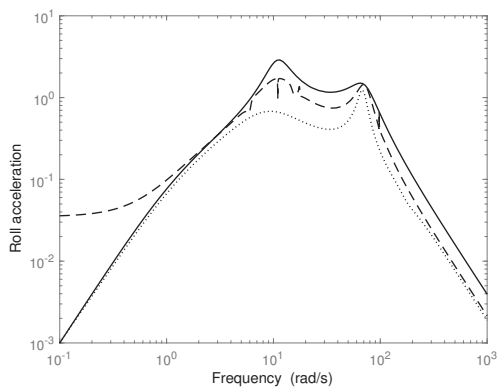


Figure 5.6. *Roll acceleration frequency response magnitudes of passive, Skyhook and active designed by solving Problem 3.1 suspension systems to the roll input: (solid) passive, (dashed) Skyhook and (dotted) active.*

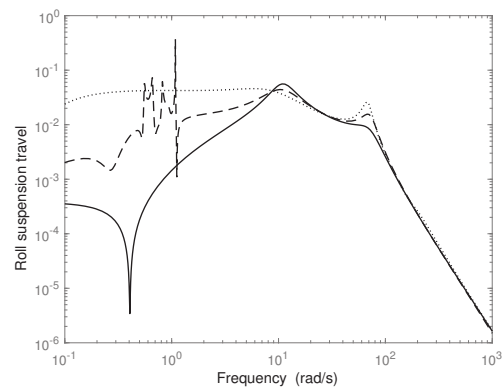


Figure 5.7. *Roll suspension travel frequency response magnitudes of passive, Skyhook and active designed by solving Problem 3.1 suspension systems to the roll input: (solid) passive, (dashed) Skyhook and (dotted) active.*

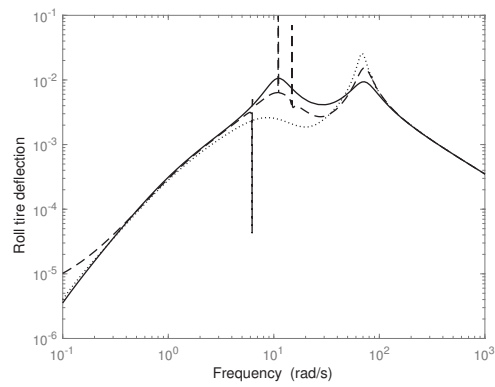


Figure 5.8. Roll tire deflection frequency response magnitudes of passive, Skyhook and active designed by solving Problem 3.1 suspension systems to the roll input: (solid) passive, (dashed) Skyhook and (dotted) active.

6. CONCLUSION AND FUTURE WORK

In this thesis, an active suspension optimal control techniques have been presented and the behavior of an active suspended vehicle using these techniques has been assessed, which achieved a good trade-off between ride comfort and drive safety. However, the active control laws are realized by force actuators which consume much energy. Motivated by the demand of energy saving, a semi active suspension control techniques have been proposed where the semi active control laws are realized by MR shock absorbers which are less energy-consumed compared to force actuators. The classical semi active suspension controls have been studied (skyhook, groundhook and hybrid control) and the frequency responses for each semi active control method has been plotted in order to gain a deep understanding of how every frequency component affects the performance indices. The results were as it has been expected, the skyhook control improve the ride comfort since it focuses on sprung mass, the groundhook control enhances the drive safety since it focuses on unsprung masses, and the hybrid control offers the advantages of both latter methods. The values of MR damping coefficients play a crucial role in the suspension system's performance, where in literature a systematic method to compute these coefficients has not been clarified. The LMI optimization has been very popular among control systems in recent years, it has been utilized for active suspension system but according to author's knowledge it has not been exploited for semi active suspension system. So, this work highlighted the feasibility and advantages of using LMI to obtain the MR damping coefficients. Since the concern is on ride comfort, the skyhook control has been optimized by LMI. The ideal skyhook configuration was optimized and then the resulted coefficients were synthesized to practical configuration. The results of the optimized conventional skyhook control were satisfied in respect to ride comfort but at expense of drive safety which resulted in excessive suspension bottoming and interrupted contact of wheels to road surface. The latter drawbacks

were the driving force for searching an alternative skyhook control to improve drive safety. The optimized alternative skyhook control therefore mitigated the contradiction between ride comfort and drive safety which prevented an excessive suspension bottoming. The alternative skyhook control improved the drive safety compared to its conventional counterpart where the suspension system requirements (minimizing the vehicle body accelerations, the dynamic tire load and the suspension travels) have been achieved.

The future work will focus on finding a remedy to improve road holding criteria of the comfort oriented semi active suspension, one remedy is such using another semi active configuration which has studied in (Koch et al., 2011), where a low bandwidth actuator has been added in series to the passive spring to realize a time varying stiffness and damping suspension system. The exploiting of LMI optimization for the latter configuration is promising enough to find an optimized results such that the road holding criteria will not be deteriorated as well as the ride comfort criteria.

REFERENCES

- Abramov, S., Mannan, S., and Durieux, O. (2009). Semi-active suspension system simulation using simulink. *International Journal of Engineering Systems Modelling and Simulation* 1(2/3), 101–114.
- Blanchard, E.D. (2003). On the control aspects of semiactive suspensions for automobile applications. Ph.D. thesis. Virginia Tech.
- Canale, M., Milanese, M., and Novara, C. (2006). Semi-active suspension control using “fast” model-predictive techniques. *IEEE Transactions on control systems technology* 14(6), 1034–1046.
- Caverly, R.J., and Forbes, J.R. (2019). Lmi properties and applications in systems, stability, and control theory. *arXiv preprint arXiv:1903.08599* .
- Chai, L., and Sun, T. (2010). The design of lqg controller for active suspension based on analytic hierarchy process. *Mathematical Problems in Engineering* 2010.
- Chen, H., and Guo, K.H. (2005). Constrained h_∞ control of active suspensions: an lmi approach. *IEEE Transactions on Control Systems Technology* 13(3), 412–421.
- Chilali, M., and Gahinet, P. (1996). h_∞ design with pole placement constraints: an lmi approach. *IEEE Transactions on automatic control* 41(3), 358–367.
- De Oliveira, M.C., Geromel, J.C., and Bernussou, J. (2002). Extended h_2 and h_∞ norm characterizations and controller parametrizations for discrete-time systems. *International Journal of Control* 75(9), 666–679.
- Du, H., Sze, K.Y., and Lam, J. (2005). Semi-active h_∞ control of vehicle suspension with magneto-rheological dampers. *Journal of Sound and Vibration* 283(3-5), 981–996.

- Esmailzadeh, E., and Fahimi, F. (1997). Optimal adaptive active suspensions for a full car model. *Vehicle System Dynamics* 27(2), 89–107.
- Gahinet, P., Nemirovskii, A., Laub, A.J., and Chilali, M. (1994). The lmi control toolbox, *Decision and Control, 1994., Proceedings of the 33rd IEEE Conference on*, IEEE. pp. 2038–2041.
- Gao, H., Lam, J., and Wang, C. (2006). Multi-objective control of vehicle active suspension systems via load-dependent controllers. *Journal of Sound and Vibration* 290(3-5), 654–675.
- Goncalves, F.D. (2001). Dynamic analysis of semi-active control techniques for vehicle applications. Ph.D. thesis. Virginia Tech.
- Ihsan, S., Faris, W.F., and Ahmadian, M. (2008). Analysis of control policies and dynamic response of a q-car 2-dof semi active system. *Shock and Vibration* 15(5), 573–582.
- Karnopp, D. (1986). Theoretical limitations in active vehicle suspensions. *Vehicle System Dynamics* 15(1), 41–54.
- Koch, G., Spirk, S., Pellegrini, E., Pletschen, N., and Lohmann, B. (2011). Experimental validation of a new adaptive control approach for a hybrid suspension system, *Proceedings of the 2011 American Control Conference*, IEEE. pp. 4580–4585.
- Kruczek, A., and Stribrsky, A. (2004). h_∞ control of automotive active suspension with linear motor. *IFAC Proceedings Volumes* 37(14), 365–370.
- Liu, Y., Waters, T., and Brennan, M. (2005). A comparison of semi-active damping control strategies for vibration isolation of harmonic disturbances. *Journal of Sound and Vibration* 280(1-2), 21–39.
- Löfberg, J. (2004). Yalmip: A toolbox for modeling and optimization in matlab, *Proceedings of the CACSD Conference*, Taipei, Taiwan.

- Murray, R.M. (2009). Optimization-based control. *California Institute of Technology, CA*.
- Ogata, K., et al. (1995). Discrete-time control systems. volume 2. Prentice Hall Englewood Cliffs, NJ.
- Poussot-Vassal, C., Sename, O., Dugard, L., Gaspar, P., Szabo, Z., and Bokor, J. (2008). A new semi-active suspension control strategy through lpv technique. *Control Engineering Practice* 16(12), 1519–1534.
- Poussot-Vassal, C., Sename, O., Dugard, L., Ramirez-Mendoza, R., and Flores, L. (2006). Optimal skyhook control for semi-active suspensions. *IFAC Proceedings Volumes* 39(16), 608–613.
- Rizvi, S.M.H., Abid, M., Khan, A.Q., Satti, S.G., and Latif, J. (2018). h_∞ control of 8 degrees of freedom vehicle active suspension system. *Journal of King Saud University-Engineering Sciences* 30(2), 161–169.
- Rubió-Massegú, J., Rossell, J.M., Karimi, H.R., and Palacios-Quinonero, F. (2013). Static output-feedback control under information structure constraints. *Automatica* 49(1), 313–316.
- Sammier, D., Sename, O., and Dugard, L. (2003). Skyhook and h_∞ control of semi-active suspensions: some practical aspects. *Vehicle System Dynamics* 39(4), 279–308.
- Savaresi, S.M., Poussot-Vassal, C., Spelta, C., Sename, O., and Dugard, L. (2010). Semi-active suspension control design for vehicles. Elsevier.
- Scherer, C., Gahinet, P., and Chilali, M. (1997). Multiobjective output-feedback control via lmi optimization. *IEEE Transactions on automatic control* 42(7), 896–911.
- Scherer, C., and Weiland, S. (2000). Linear matrix inequalities in control. *Lecture Notes, Dutch Institute for Systems and Control, Delft, The Netherlands* 3(2).

- Skogestad, S., and Postlethwaite, I. (2007). Multivariable feedback control: analysis and design. volume 2. Wiley New York.
- for Standardization, I.O. (1997). ISO catalogue. International Organization for Standardization.
- Taghirad, H.D., and Esmailzadeh, E. (1998). Automobile passenger comfort assured through lqg/lqr active suspension. *Journal of vibration and control* 4(5), 603–618.
- Türkay, S., and Akçay, H. (2005). A study of random vibration characteristics of the quarter-car model. *Journal of sound and vibration* 282(1-2), 111–124.
- Türkay, S., and Akçay, H. (2010). Tire damping effect on h_2 optimal control of half-car active suspensions. *Journal of Vibration and Acoustics* 132(2), 024502.
- Türkay, S., and Akçay, H. (2014). Multi-objective control of a full-car model using linear-matrix-inequalities and fixed-order optimisation. *Vehicle System Dynamics* 52(3), 429–448.
- Zames, G. (1981). Feedback and optimal sensitivity: Model reference transformations, multiplicative seminorms, and approximate inverses. *IEEE Transactions on automatic control* 26(2), 301–320.